

UNIVERSITA' DEGLI STUDI DI MILANO

PhD Course in Pharmacological Sciences

XXVIII CYCLE



**Positive modulation of mGlu5 reverses ASD-like behaviors found in *SHANK3* knock-out mice**

Coordinator: Prof. Alberto Corsini

Tutor: Prof. Maria Elvina Sala

Co-Tutor: Dr. Carlo Sala

PhD Thesis of :  
**Cinzia Vicidomini**  
R10230

Academic Year 2014/2015

# ***INTRODUCTION***

## **SYNAPSES**

The term synapse describes the specialized zone of functional contact between neurons, through which nerve cells can communicate with each others (Kandel, 2013).

The presynaptic neuron is the one that transmits signals, the postsynaptic neuron is the one that receives information. There are two different types of synapses: electrical and chemical.

Chemical synapses are more abundant then electrical ones and convey the electrical signals indirectly via biochemical agents (neurotransmitters) whereas electrical synapses convey the electrical signal directly via ion channels (known as gap junctions).

For this reason signal transduction occurs faster at electrical synapses but is much less modifiable compare to chemical synapses.

In this study we will focus our attention on chemical synapses, so all of the following information refer to this type of synapses.

Transmission across chemical synapses is mediated by two different neurotransmitters, that are glutamate in the excitatory synapses and  $\gamma$ -aminobutyric acid (GABA) in the inhibitory ones.

## **EXCITATORY SYNAPSES**

Excitatory glutamatergic synapses represent the vast majority of the synapses involved in central neuronal communication.

A typical characteristic of these synapses is the presence of a prominent post synaptic density (PSD), an electron dense thickening of the postsynaptic membrane, containing glutamate receptors, scaffold proteins, cytoskeletal molecules and signal transduction molecules (Sheng and Hoogenraad, 2007). On most principal neurons in the mammalian brain the PSD is localized on tiny actin rich protrusions, called dendritic spines (Sheng and Hoogenraad, 2007). Dendritic spines are small (0.5-2  $\mu\text{m}$  of length) motile protrusions that receive synaptic contacts from glutamate-releasing axons. They contain all the essential postsynaptic components, including

the PSD, actin cytoskeleton and various membranous organelles such as the endoplasmic reticulum (ER) and endosomes.

Typical mature spine has a bulbous head (receiving a single synapse) that is connected to the dendrite through a thin spine neck (**Figure A**) (Sheng and Hoogenraad, 2007).

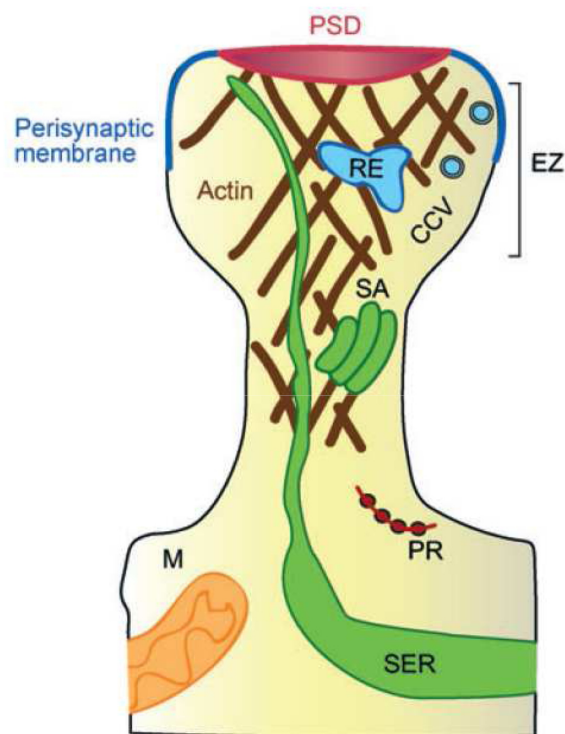


### **Figure A: Microanatomy of dendritic spine**

Schematic representation of mature mushroom-shaped spine, in which are shown the PSD, the perisynaptic membrane and others organelles (Sheng and Hoogenraad, 2007).

Due to its architecture and molecular organization, spine isolates the synapse from the rest of the dendrite creating in this way a microdomain as regards protein trafficking, ion release and downstream signaling.

The number, size and shape of spines are subjected to plastic changes during development stages, allowing to long-term modification of synaptic strength (Sorra and Harris, 2000) (Sheng and Hoogenraad, 2007, Sheng and Kim, 2011).

Spines shape has been categorized as “mushroom”, “thin” or “stubby” by Sheng

and Hoogenraad (Sheng and Hoogenraad, 2007), but in 2014 two others additional categories have been added: branched and cup-shaped spines (Ebrahimi and Okabe, 2014). The typical shape of a mature spine is the mushroom one, with a thin neck and a bulbous head (Sala et al., 2001). The shape, size and stability of spines depend on actin, that is the primary cytoskeleton within spines. There is a complex network of regulatory proteins, including Rho family GTPase, that control actin rearrangements (Tada and Sheng, 2006, Ethell and Pasquale, 2005).

Several hundred proteins have been found at PSD; In particular PSD proteins are involved in cellular communication and signal transduction (adhesion, GTPases, kinase/phosphates, receptors, and channels), cellular organization (cytoskeleton, membrane traffic, motors, and scaffolds), energy (mitochondria and metabolism), protein synthesis and processing (translation and chaperones), and others (**Figure B**).

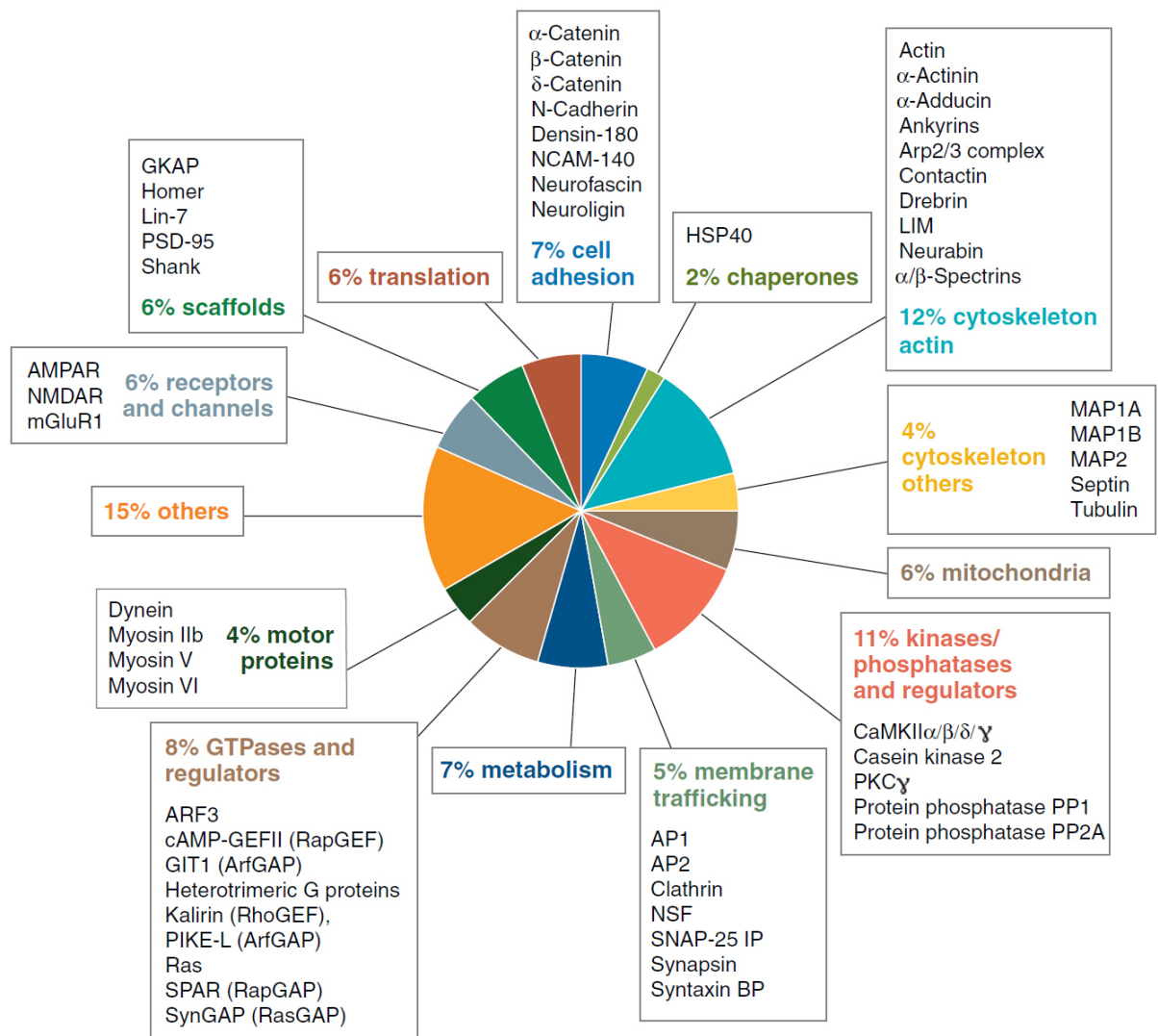


## **Figure B: Protein composition of the PSD fraction**

Chart showing the variety of proteins found in the PSD fraction of the forebrain, grouped according to cellular function. PSD proteins are involved in cellular communication and signal transduction, cellular organization, energy, protein synthesis and processing (Sheng and Hoogenraad, 2007).

These membrane proteins are assembled into a disk-like proteinaceous structure, ~300–400 nm wide and ~30–50 nm thick (Sheng and Hoogenraad, 2007).

In addition to the PSD, the postsynaptic compartment also owns perisynaptic and extrasynaptic regions with highly specialized functions (Okabe, 2007, Harris and Weinberg, 2012) containing a distinctive set of proteins, such as metabotropic glutamate receptors (mGlu receptors) (Okabe, 2007, Harris and Weinberg, 2012), proteins involved in endocytosis and low levels of ionotropic glutamate receptors.

## **GLUTAMATE RECEPTORS**

Glutamate is the main excitatory neurotransmitter that can activate different types of glutamate receptors.

Glutamate receptors can be classified in two groups depending on the mechanism by which their activation gives rise to a postsynaptic current.

These two groups are: ionotropic receptors and metabotropic receptors.

## **IONOTROPIC RECEPTORS**

Ionotropic receptors are non-selective cation channels that allow the passage of  $\text{Na}^+$ ,  $\text{K}^+$  and in some cases  $\text{Ca}^{2+}$ , in response to their activation by glutamate; for this reason iGluRs mediate fast synaptic transmission.

Depending on the selective agonist that activates iGluRs it is possible to group them in N-methyl-D-aspartate receptors (NMDARs),  $\alpha$ -amino-3-hydroxy-5-methyl-4-isoxazolepropionic acid receptors (AMPA receptors) and 2-carboxy-3-carboxymethyl-4-isopropenylpyrrolidine (Kainate) receptors (KARs) (Kew and Kemp, 2005, Bigge, 1999).

## ■NMDA receptors

The NMDA subfamily of glutamate receptors forms multisubunit, nonselective cation channels similar to most other ligand-gated ion channel receptors (Kandel, 2013).

NMDA receptors allow the entry of  $\text{Ca}^{2+}$  in addition to monovalent cations like  $\text{Na}^+$  and  $\text{K}^+$ .

This characteristic can produce an increase of the concentration of  $\text{Ca}^{2+}$  in the postsynaptic neuron and the  $\text{Ca}^{2+}$  concentration change can then acts as a second messenger to activate intracellular signaling cascades (MacDermott et al., 1986).

Other two unique properties of this class of receptors are that opening the channel requires the presence of a co-agonist (the amino acid glycine), and that extracellular  $\text{Mg}^{2+}$  acts as a voltage dependent 'pore blocker', blocking the channel at hyperpolarized, but not depolarized, voltages (Kandel, 2013).

There are at least 7 different subunits of NMDA receptors: GluN1, GluN2A-D and GluN3A-B. Their activation requires the assembly of one obligatory GluN1 subunit and one of the GluN2 or GluN3 subunits (Okabe, 2007, Bigge, 1999, Kew and Kemp, 2005).

NMDA receptors are ubiquitously distributed throughout the central nervous system (CNS). They are located mainly postsynaptically, but some of them are present on presynaptic membranes.

## ■AMPA receptors

AMPA receptors are widely expressed in the mammalian CNS and mediate fast excitatory neurotransmission in response to glutamate binding (Niciu et al., 2012) but their prolonged activation is highly neurotoxic (Szczurowska and Mareš, 2013).

This class of receptors are homo- or heterotetramers composed of a four subunit family (GluA1–4 also called GluA-D) (Bigge, 1999). GluA2 subunit makes AMPARs not permeable to  $\text{Ca}^{2+}$  and drastically decreases their conductance, making the GluA2 a critical subunit for the regulation of synaptic AMPAR signaling (Bigge, 1999, Kew and Kemp, 2005). AMPA receptors different subunits are characterized by a transmembrane and an extracellular domains, that are very similar, indeed they differ only for the cytoplasmic intracellular tail. Thanks to the diversity of the intracellular tail each subunit of AMPARs interacts with different proteins.

The majority of the proteins that interact with AMPARs presents one or more PDZ domains, able to bind to the C-terminal intracellular tail of the AMPA subunits (Sala et al., 2001).

The altered functions of AMPA receptors have been implicated in many neurological and psychiatric diseases, which make these receptors an attractive drug target (Cheng et al., 2012).

#### ■ KAINATE RECEPTORS (KARs)

This class of receptors is composed of two related subunit families, GluK1-5. They are tetrameric complexes that are widely expressed in the CNS and appear to be involved in the functioning of many neural networks.

### METABOTROPIC RECEPTORS

In addition to causing a fast excitatory synaptic responses, glutamate has important neuromodulatory effects by the activation of G protein-coupled receptors (GPCRs) named metabotropic glutamate (mGlu) receptors (Chen et al., 2007).

Like all G-protein coupled receptors, metabotropic glutamate receptors are seven transmembrane domains spanning receptors with an extracellular N-terminus and intracellular C-terminus (Niciu et al., 2012).

This family of receptors includes eight subtypes termed mGlu1 to mGlu8 receptors, that are grouped in three different classes based on sequence homology, primary G protein coupling and pharmacological properties (Chen et al., 2007).

These metabotropic receptors, which modulate postsynaptic ion channels indirectly, differ in their coupling to intracellular signal transduction pathways and in their sensitivity to pharmacological agents.

#### ■ GROUP I

All the members (mGlu1 and mGlu5) are coupled to Gq/11 G-proteins and are primarily localized to perisynaptic ring (Sheng and Hoogenraad, 2007) (Chen et al., 2007).

mGlu5 receptors have a broad distribution within the CNS, with moderate to high expression levels in the cerebral cortex, dorsal and ventral striatum and hippocampus (Cleva and Olive, 2011), while mGlu1 is highly expressed in purkinje cells of the cerebellar cortex, in most of the thalamic nuclei, in the superior colliculus and in the hippocampus (Martin et al., 1992, Hubert et al., 2001).

The stimulation of these receptors causes the activation of the associated enzyme phospholipase C, which hydrolyzes phosphoinositide phospholipids in the cell's plasma membrane (Bonsi et al., 2005). As consequence inositol 1,4,5-trisphosphate (IP3) and diacyl glycerol are produced. Due to its hydrophilic character, IP3 reaches the endoplasmic reticulum, where it induces, by binding to its receptor, the opening of calcium channels increasing in this way the cytosolic calcium concentration (Chu and Hablitz, 2000, Bonsi et al., 2005, Bates et al., 2002). The lipophilic diacylglycerol remains in the membrane, acting as a cofactor for the activation of protein kinase C (Niciu et al., 2012).

Activation of Group I mGlu receptors results in the activation of many intracellular signaling molecules such as protein kinase A (PKA), mitogen-activated protein kinase (MAPK), extracellular signal-related kinase (ERK), and cAMP response element binding protein (CREB) (Cleva and Olive, 2011).

Interestingly, group I mGlu receptors are physically coupled to NMDA receptors through different proteins, including PSD-95, Shank, Homer, as well as through a direct interaction (Perroy et al., 2008).

Group I of metabotropic receptors are also biochemically coupled to NMDA receptor function via PKC.

So activation of these receptors causes an enhanced functionality of the NMDA receptors (Attucci et al., 2001, Rosenbrock et al., 2010).

## ■GROUP II

mGlu2 and 3 inhibit via Gi the adenylyl cyclase activity and are situated in presynaptic axon terminals where they modulate glutamate release (Cartmell and Schoepp, 2000, Thomas et al., 2001)

### ■GROUP III

mGlu4, mGlu6, mGlu7 and mGlu8 combine with Gi and they are mainly localized at the axon terminals.

Metabotropic glutamate (mGlu) receptors have been suggested to play a role in neuropsychiatric disorders including schizophrenia, drug abuse, and depression (Halberstadt et al., 2011).

In addition, recently have been published different data reporting that rare genetic variation in the group I of metabotropic glutamate-receptor signaling pathway contributes to autism susceptibility (Kelleher et al., 2012).

D'Antoni and colleagues reported that both an increased and reduced mGlu5 functioning is related to ID and ASD (D'Antoni et al., 2014).

For example the analysis of  $Fmr1^{-Y}$  mouse, a model of Fragile X, that is the most common inherited cause of autism, has shown excessive mGlu5-dependent synaptic protein synthesis and plasticity (Bear et al., 2004).

On the contrary in several mouse models of tuberous sclerosis syndrome (TSC), a genetic syndrome associated to ASD and ID, have been reported a decreased mGlu5 mediated LTD.

Furthermore the association of mGlu5 alterations to ASD an ID is provided also by our previous *in vitro* data, in which we knocked down all the major Shank3 isoforms through RNA interference and we observed a dysfunctional mGlu5 mediated signaling. Our results suggest a possible role of mGlu5 signaling in the pathophysiology of Phelan McDermid Syndrome, that is a rare genetic disorder that causes a severe form of intellectual disability (ID), expressive language delays and other autistic features (Verpelli et al., 2011).

Concluding many evidences underlie the involvement of group I of mGlu receptor signalling, in several disorders associated to ID and autism, suggesting that these receptors may be targeted by therapeutical interventions in different neuropsychiatric disorders (D'Antoni et al., 2014).

## POSITIVE ALLOSTERIC MODULATORS (PAMs) OF mGlu5 RECEPTORS

Positive allosteric modulators (PAMs) of mGlu5 receptors were developed to increase NMDA receptor function in order to ameliorate some cognitive deficits associated to schizophrenia, as there are some evidences that NMDA hypofunction causes cognitive problems in this disorder (Chen et al., 2007, Conn et al., 2009, Marino and Conn, 2002, Conn et al., 2008).

Compare to PAMs, the classical orthosteric agonists of mGlu5, such as (S)-3,5-dihydroxyphenylglycine (DHPG) and 2-chloro-5-hydroxyphenylglycine (CHPG) offer poor discrimination between receptors subtypes, because of the high degree of sequence homology of glutamate binding site, have poor brain barrier permeability and cause a rapid desensitization of the receptors (Cleva and Olive, 2011).

On the contrary PAMs are able to bind the receptors at a different site and to increase their function in presence of the endogenous ligand (glutamate).

One of the best characterized PAM is 3-Cyano-*N*-(1,3-diphenyl-1*H*-pyrazol-5-yl)benzamide (CDPPB) and is the first one able to penetrate brain barrier.

During the last years have been reported different studies demonstrating that CDPPB treatment is able to ameliorates cognitive deficits associated to different neuropsychiatric disorders (Cleva and Olive, 2011).

In *Tsc2* heterozygous mice, a model of of tuberousclerosis syndrome (TSC), a genetic syndrome associated to ASD and ID, the treatment with CDPPB is able to restore mGlu5 mediated LTD (Auerbach et al., 2011).

In a mouse model lacking exon 4-6 of *SHANK2* gene, that presents ASD-like phenotypes, the treatment with CDPPB normalizes some behavioral deficits (Won et al., 2012).

Finally, treating with CDPPB primary rat neurons knocked down for Shank3, we were able to rescue the altered mGlu5 mediated synaptic signalling (Verpelli et al., 2011).

Considering the therapeutic potential of PAMs to treat different neuropsychiatric disorders is not surprising that, at the moment different research groups are performing many studies to improve the pharmacological characteristics of these compounds.

For example in 2015 have been identified VU0409551 as a novel mGlu<sub>5</sub> PAM that exhibits distinct stimulus bias and selectively potentiates mGlu<sub>5</sub> coupling to G<sub>αq</sub>-

mediated signaling but not mGlu<sub>5</sub> modulation of NMDAR currents or NMDAR-dependent synaptic plasticity (Rook et al., 2015).

VU0361747, is another mGlu<sub>5</sub> PAM optimized to eliminate allosteric agonist activity. It has robust in vivo efficacy and does not induce adverse effects at doses that yield high brain concentrations (Rook et al., 2013).

Summarizing, the group I of mGlu receptors may represent a potential target for therapeutic interventions in some forms of neurodevelopmental disorders, such as ASD and the use of PAM could ameliorate different behavioral deficits associated to these disorders.

## **SCAFFOLD PROTEINS**

Scaffolding component of the PSD represents a particular focus for the present study. This scaffolding component is characterized by proteins equipped with protein-protein interaction domains holding all molecules of the PSD and ensuring its assembly and functionality. One of the most important classes of scaffold proteins is the family of Shank proteins.

### **SHANKs**

The ProSAP/Shank family of proteins contains three members all localized at the postsynaptic density level of excitatory synapses: Shank1 (Shank1a, Synamon or SSTRIP), ProSAP1/Shank2 (CortBP1) and ProSAP2/Shank3.

The name ProSAP is due to the proline-rich clusters that are conserved among all the family members (Boeckers et al., 1999), the other term, Shank, was given by Naisbitt and colleagues (Naisbitt et al., 1999) and is referred to the SH3 domain and to the multiple ankyrin repeats present in this family of proteins.

Shanks are large proteins with a molecular weight of more than 180KDa (Boeckers et al., 1999).

All the family members present different domains for specific protein-protein interactions and the presence of multiple domains within a single polypeptide is typical of scaffold proteins (Sheng and Kim, 2000).

All Shank proteins contain from N-terminal to C-terminal, the following five well-conserved domains: an N-terminal ankyrin repeats, an SH3 domain, a PDZ domain, a proline-rich domain, and a sterile alpha motif (SAM) domain (**Figure C**).

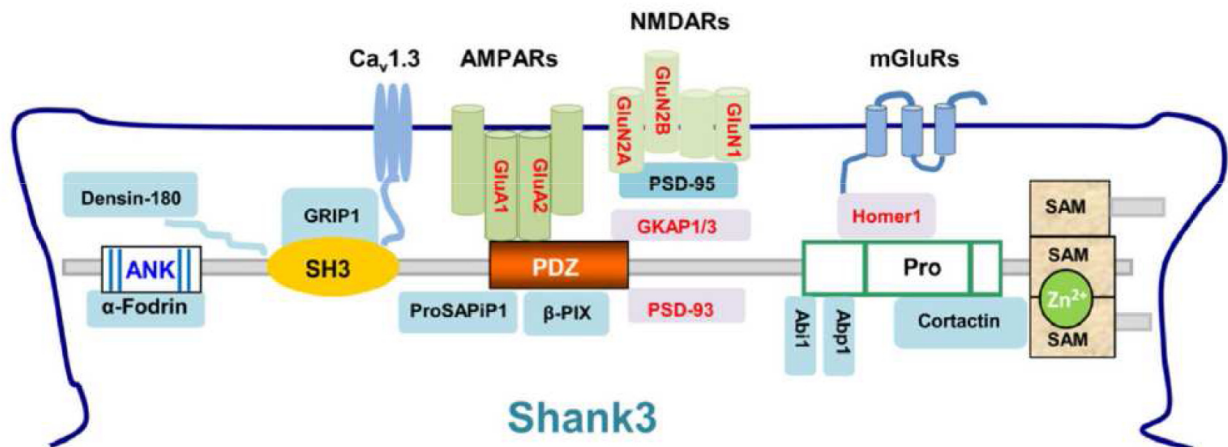


**Figure C: Shank protein domains structure**

Cartoon in which is shown the domain composition of Shank proteins. For each domain are listed the binding partners (Jiang and Ehlers, 2013).

-N-terminal ankirin domain (ANK) mediates the binding to  $\alpha$ -Fodrin and Sharpin.

$\alpha$ -Fodrin is one of the major constituent of the PSD and interacts with actin and with calmodulin. The interaction between ANK domain and  $\alpha$ -Fodrin connects PSD to the cytoskeleton.

Sharpin is a subunit of ubiquitin chain assembly complex, which is essential for the activation of Nf-kB signalling. Nf-kb is a transcription factor that is activated in synapses in response to excitatory synaptic transmission and plays an important role in different processes such as neuronal survival, memory and learning (Freudenthal et al., 2004).

-Src homology 3 (SH3) domain modulates AMPA trafficking by binding GRIP, that is another scaffold protein, containing 7 PDZ domains interacting with AMPA receptors (Sheng and Kim, 2000). Moreover the SH3 domain also binds to the voltage-gated

L-type calcium channel CaV 1.3, this interaction is important to link calcium influx to pCREB signalling (Verpelli et al., 2012).

-PDZ domain, binds the C-terminus of GKAP, which interacts with the guanylate kinase domain of PSD-95 via N-terminus, linking in this way Shank to NMDA receptor/PSD-95 complex (Sheng and Kim, 2000).

PDZ domain interacts also with ProSAP-interacting protein 2 (ProSAPiP2), that is important in the attachment and modulation of cytoskeletal elements thanks to its actin binding characteristics.

-proline rich region, contains more than 1000 residues rich in proline and serine residues and commonly acting as binding sites for SH3 and EVH1 (Sheng and Kim, 2000).

The proline-rich region of Shank is able to mediate different sets of protein interactions; in particular two proteins have been shown to bind to the proline-rich region: Cortactin and Homer.

Cortactin is an F-actin-binding protein enriched in the cell-matrix contact sites and in growth cones of neurons (Sheng and Kim, 2000).

Cortactin moves to the cell periphery in a growth-factor and Rac-1 dependent manner and it redistributes to synapses in response to glutamate stimulation (Naisbitt et al., 1999).

Thus Cortactin plays an important role in regulating the organization of actin cytoskeleton in the cell cortex and in dendritic spines.

-SAM domain, is important for the localization of Shank proteins at the PSD. This domain allows self-multimerization via tail tail interaction, in particular this self-multimerization can be regulated by Zn<sup>2+</sup> ions for Shank2 and 3 (Naisbitt et al., 1999, Gundelfinger et al., 2006, Grabrucker et al., 2011a).

The Shank family members show a distinct pattern of expression: Shank1 is expressed almost exclusively in the brain; Shank2 is strongly expressed in the brain but is present also in non-neuronal tissues, like kidney and liver. Shank3 is highly expressed in brain, heart and spleen (Sala et al., 2015).

All three family members are highly expressed in the hippocampus and cortex, whereas Shank3, but not Shank1 or Shank2, is highly expressed in the striatum (Verpelli et al., 2012).

As mentioned above Shank proteins interact with different glutamate receptors.

In this study we will focus on the interaction between Shank3 and the group I of metabotropic receptors, which includes mGlu5.

The binding between mGlu5 and Shank3 is ensured by the association of the proline rich domain of Shank3 to another scaffold protein named Homer1.

## HOMER PROTEINS

Homer proteins (Homer 1, 2, 3) are a family of scaffold proteins, that participate to different neuronal processes, ranging from calcium homeostasis to synaptic plasticity (Foa and Gasperini, 2009).

They present an N-terminal enabled/vasodilator-stimulated phosphoprotein homology domain (EVH1) and a C-terminal coiled-coil (CC) domain.

The EVH1 domain is involved in the binding to synaptic signalling ligands, such as the metabotropic glutamate receptor (mGlu), the inositol tri-phosphate (IP3R) and the ryanodine receptors (RyR), and other scaffold proteins like Shanks. (Foa and Gasperini, 2009). Thus Homer physically and functionally links type I metabotropic glutamate receptors to their downstream effectors, the IP3 receptors, allowing a more efficient release of intracellular calcium in response to receptor stimulation (Sheng and Kim, 2000).

Homer proteins possess a CC domain, which mediates homophilic and or heterophilic interactions with other members of the family. In particular Hayashi and colleagues in 2006 suggested that the native long-form Homers exist as tetrameric hubs with CC domains. The tetramerization exposes four EVH1 domains in a spatially optimized configuration for ligand binding that is required for efficient localization to dendritic spines. Thus Homer tetramers and antiparallel Shank homodimers can form multidimensional scaffolding substrate through which ligands for both proteins can be efficiently assembled (Hayashi et al., 2006).

## SHANK3 ISOFORMS

In human and rodents *SHANK* genes present a very complex transcriptional regulation with multiple intragenic promoters and alternative spliced exons (Jiang and Ehlers, 2013).

Transcripts of *SHANK3* are the most and best characterized compare to the other two members of the family.

Indeed in this gene the combination of multiple promoters and alternative splicing processes leads to a production of an extensive array of mRNA and protein isoforms that has not been fully characterized yet (Wang et al., 2014).

The mouse *SHANK3* gene presents 22 exons that encode a synaptic scaffolding protein with five functional domains. The alternatively spliced exons of *SHANK3* encode the SH3, proline-rich and SAM domains.

*SHANK3* contains at least five intragenic promoters both in humans and rodents, which produce specific isoforms (Shank3a-f, as described in **Figure D**) with a unique combination of different protein domains (Wang et al., 2014).

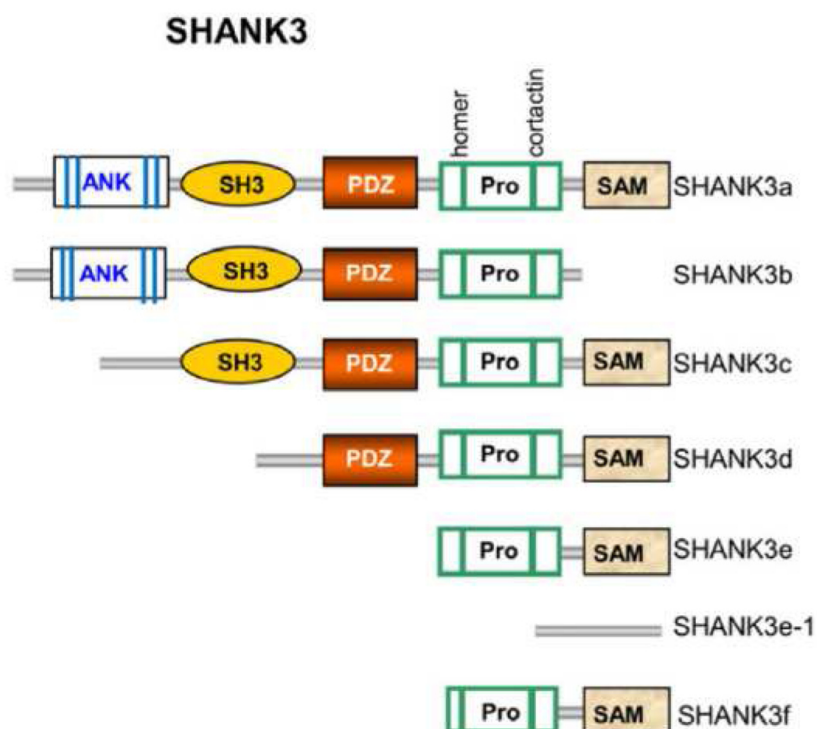


### **Figure D: Shank3 protein isoforms**

Diagram in which are shown *SHANK3* protein isoforms (*SHANK3* a-f). Protein domain structures were obtained from confirmed mRNA expressed from different promoters in human and mouse brains (Jiang and Ehlers, 2013).

As described in detail above, each domain mediates specific protein-protein interactions so this could mean that each Shank3 isoform has a distinct set of functions.

For example Shank3e and Shank3f mRNAs lack exon encoding the PDZ, that is necessary for the interaction between Shank3 and NMDA and AMPA receptors (Naisbitt et al., 1999).

Shank3b is an isoform without the proline rich and SAM domains that are fundamental for Homer binding and for multimerization (Tu et al., 1999).

### **SHANKOPATHIES**

Considering the role of Shank proteins as master scaffolding molecules and their importance in regulating dynamic changes of synaptic morphology (Boeckers et al., 2002) it's not surprising that all members of the SHANK gene family have been linked to human "synaptopathies".

With this term are described a group of neuropsychiatric disorders, which includes autism spectrum disorder (ASD), intellectual disability (ID), schizophrenia, obsessive compulsive disorder and bipolar disorder, so called because the mutations in these disorders lead to abnormal synaptic development or function (Han et al., 2013).

Mutations and deletions in *SHANK* genes are so much involved in the generation of neurological disorders that has been coined a specific term to indicate diseases in which *SHANK* is impaired: the "Shankopathies".

This definition includes different pathologies such as ASD, schizophrenia and Alzheimer disease. Within all ASDs, the most common Shankopathy is the Phelan McDermid Syndrome (PMS or 22q13.3 deletion syndrome) (Carbonetto, 2014).

## PHELAN-MCDERMID SYNDROME

Phelan-McDermid syndrome, also called PMS or 22q13.3 deletion syndrome, is a neurodevelopmental disorder, caused by a deletion in the terminal end of the long arm of chromosome 22. The size of the deletion leading to PMS can range from <100kb to >9Mb and these deletions cause the haploinsufficiency of four genes *ACR*, *RABL2B*, *MGC70863* and *SHANK3* (Guilmatre et al., 2014).

The first evidence of the involvement of *SHANK3* gene in the pathogenesis of PMS was reported in 2001 by Bonaglia and colleagues that identified a patient with a translocation between chromosome 12 and 22 (affecting only *SHANK3*), who presented the main symptoms of Phelan-McDermid Syndrome (Bonaglia et al., 2001). In 2006 Wilson et al. found that 56 patients affected by PMS, presented a loss of 1 copy of *SHANK3* gene (Wilson et al., 2003). After these two studies many others evidences documented that small deletions and mutations, that affect only *SHANK3*, caused similar phenotypes including ASD and ID (Durand et al., 2007, Boccuto et al., 2013). In addition de novo sequence changes including missense, frame shift and splice site mutations have been identified in *SHANK3* gene of ASD patients (Dhar et al., 2010, Boccuto et al., 2013, Moessner et al., 2007, Uchino and Waga, 2013).

The genomic rearrangements identified in patients with PMS can range from simple 22q13 deletions (72%), ring chromosomes (14%), unbalanced translocation (7%), to interstitial deletions, all resulting in haploinsufficiency of *SHANK3* gene (Leblond et al., 2014). The unbalance translocation can be inherited or de novo, in 80-85% of individuals, or from others structural rearrangements involving chromosome 22, in 15-20% of cases. Previous studies reported conflicting results from genotype-phenotype correlations but now there are some new evidences that larger deletion sizes, which involved more genes, are associated with more severe phenotypes (Soorya et al., 2013, Dhar et al., 2010).

The true incidence of PMS is unknown, and this is due to problems in diagnosis both at laboratory and clinical levels.

The clinical features of PMS are heterogeneous, and no specific symptoms are considered pathognomonic, for this reason the diagnosis is based on genetic analysis (Costales and Kolevzon, 2015).

The identification of *SHANK3* haploinsufficiency is performed using different genetic tests, the most common is CMA followed by multiplex ligation-dependent amplification to confirm the relative gene copy number (Schouten et al., 2002).

The CMA analysis is not useful to identify the very small intragenic deletions (<30kb) and the mutations of the gene; in these cases DNA sequencing techniques, to evaluate individual base pairs within the gene, are required (Peters et al., 2015).

Although PMS is characterized by heterogeneous clinical symptoms, the most common features of the syndrome include neonatal hypotonia, moderate to severe intellectual impairment, absent or delayed speech and normal growth (Phelan et al., 2001). Developmental delays can't appear during the first 12 months of life but a common symptom is the neonatal hypotonia that can contribute to poor feeding, weak cry, poor head control and delayed motor milestones, like crawling and walking (Phelan et al., 2001, Sarasua et al., 2014). 75% of patients affected by PMS shows language delays; in particular expressive language is more affected than receptive language (Phelan and McDermid, 2012). Differently to other autosomal chromosome abnormalities, that are associated with growth deficiency, patients affected by 22q13.3 deletion syndrome have a normal range of growth. Different studies report a wide range of ASD prevalence in PMS (Bonaglia et al., 2001, Phelan et al., 2001, Sykes et al., 2009); in addition patients with PMS are commonly affected by ID, in particular 75% of individuals show severe-to-profound intellectual deficits (Soorya et al., 2013). Other common symptoms of PMS are various dysmorphic features such as ear abnormalities, bulbous nose, long eyelashes, large and fleshy hands, dysplastic toenails (**Figure E**). However the facial features most likely associated with deletion size, makes it difficult to diagnose this syndrome exclusively from the facial phenotype (Soorya et al., 2013, Costales and Kolevzon, 2015).



**Figure E: Patients affected by PMS**

Patients affected by PMS show wide differences in facial phenotypes, that may create clinical diagnosis difficulties (Phelan and McDermid, 2012).

## PHELAN-MC DERMID TREATMENTS

The only approaches to treat PMS at the moment are speech, occupational, physical and behavioral therapies. In addition the medical follow up is important to detect medical and psychiatric comorbidities.

Only three clinical studies have been reported to treat PMS.

The first one regards the use of intranasal insulin, which has been involved in synaptic plasticity in neuronal model and has ameliorated memory in patients affected by Alzheimer disease (Reger et al., 2009). In 6 patients treated 3 times daily for 12 months have been observed beneficial effects on cognitive function and motor development without adverse effects on glucose levels (Schmidt et al., 2009).

The second clinical study regards the use of two second generation of antipsychotics, risperidone and more recently aripipazole, that have been approved

for symptomatic treatment of ASD. Both have been demonstrated to be effective in reducing maladaptive behaviors, e.g. irritability, that so often interfere with daily living activities and educational approaches (Canitano, 2014).

The third possible approach is based on the use of Insulin-like growth factor 1 (IGF-1), a small polypeptide, that crosses the blood–brain barrier and is important in regulating synapse formation, neurotransmitter release and neuronal excitability via posttranslational modification of NMDA and AMPA receptors. The treatment of Shank3-deficient mice with IGF-1 improved AMPA receptor-mediated transmission, rescued cellular long-term potentiation and had beneficial effects on motor skills (Bozdagi et al., 2013). IGF-1 has been used also to treat pluripotent stem cells (iPS) derived from patients affected by PMS and resulted in improved NMDA- and AMPA-mediated responses (Shcheglovitov et al., 2013).

The first clinical study of IGF-1 administration in patients with PMS is currently underway, and preliminary results suggest tolerability and significant improvements in both social impairments and restrictive behaviors (Costales and Kolevzon, 2015).

During these years the molecular mechanisms responsible for the deficits in PMS are becoming more understood and this will open new possibility to develop new strategy to treat patients affected by *SHANK3* deletions and mutations.

## SHANK3 MOUSE MODELS

Since little is known about the pathophysiological and molecular basis of ASD, the development of animal models is an important step towards a better understanding of human genetics of ASD and towards the discovery of effective therapeutic strategies.

Mutant mice for all *SHANK* family genes have been produced, in particular seven Shank3 mutant mice have been reported (Peça et al., 2011, Schmeisser et al., 2012, Bozdagi et al., 2010, Wang et al., 2011, Kouser et al., 2013, Lee et al., 2015).

Two different laboratories generated two mouse models with the deletion of exon 4-9, lacking the ankyrin repeats:  $\Delta\text{ex4-9}^{\text{Buxbaum(A)}}$  (Bozdagi et al., 2010) and  $\Delta\text{ex4-9}^{\text{Jiang (B)}}$  (Wang et al., 2011). Two mice were generated by Peca and colleagues : one with the deletion of the exon 4-7 lacking the ankyrin repeats (*Shank3 (4-7)*) and one

with a deletion of exon 13-16 lacking the PDZ domain (*Shank3 (13-16)*) (Peça et al., 2011). There are also a mouse with an exon 11 deletion lacking the SH3 domain (*Shank3(11)*) (Schmeisser et al., 2012), a mouse with an exon 21 deletion (*Shank3 (21)*) lacking the major naturally occurring isoforms of *Shank3* (Kouser et al., 2013) and finally a mouse with an exon 9 deletion lacking the ankyrin repeat region (Lee et al., 2015).

All of the deletions in these mouse models cause a frame shift for targeted transcripts, generating a truncated Shank3 protein or possible disruption of full-length RNA or protein isoforms due to the stability of encoded mRNA or protein.

Considering that *SHANK3* gene presents multiple intragenic promoters and alternative spliced exons, each of these mice is expected to have disruption of different Shank3 isoforms (Jiang and Ehlers, 2013, Sala et al., 2015).

All the mouse models were characterized biochemically and behaviorally, and overall, the data obtained from the studies support a general conclusion that synaptic function is impaired and social behaviors are abnormal in mice with *SHANK3* deletions.

The major characteristics of each mouse model are reported in **Figure F**.

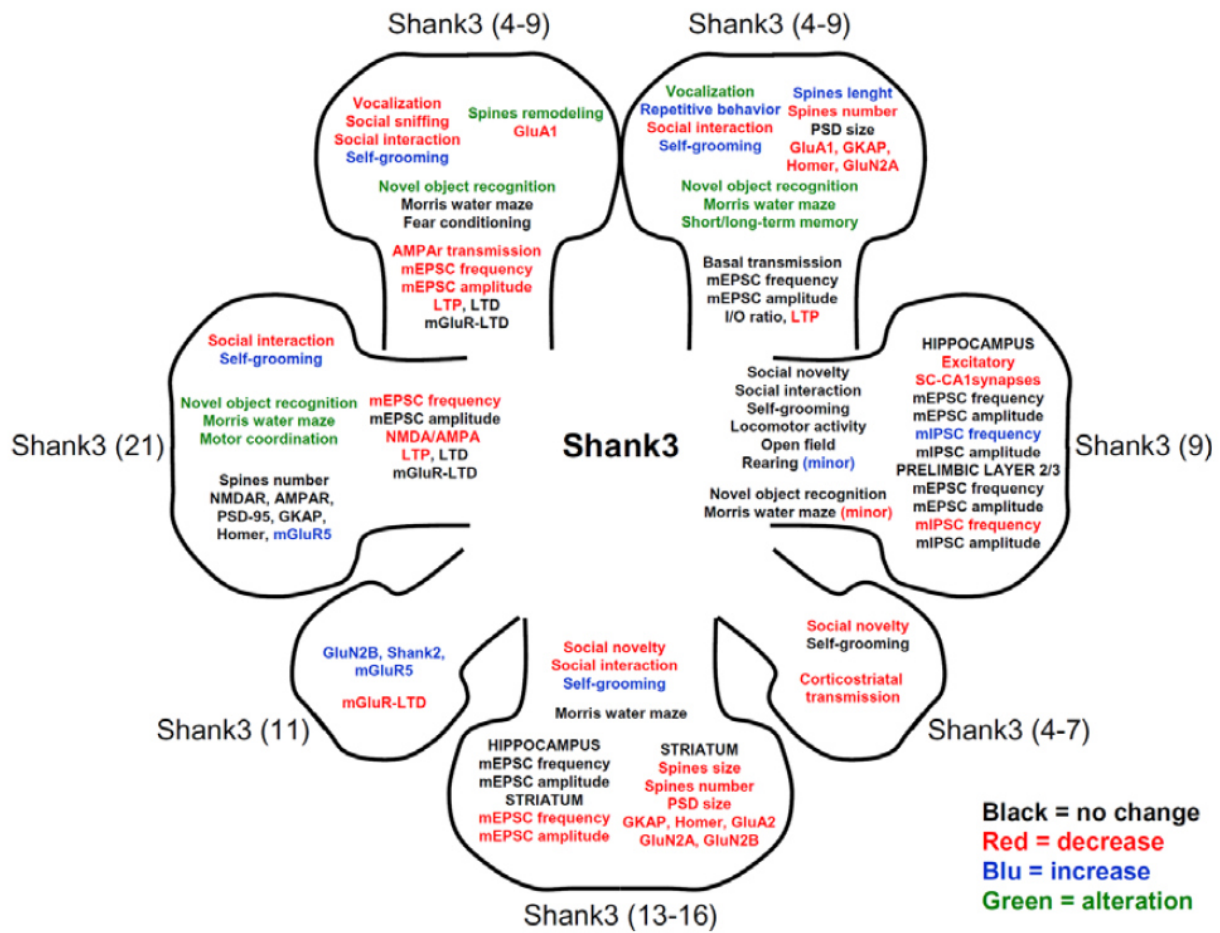


**Figure F: Behavioral, molecular and electrophysiological characteristics of Shank3 mutant mice**

Cartoon in which are reported the main deficits of different Shank3 mutant mouse models (Sala et al., 2015).

From the analyses performed on the different mouse models have been reported these main defects: repetitive and social behavior deficits, memory and learning impairments.

Repetitive behavior and generalized social deficits are typical phenotypes reported in ASD patients. Repetitive behavior in mice is represented by a self-grooming behavior.

Increased self-grooming was found in both *Shank3 (4-9)a* and *b* mice (Bozdagi et al., 2010, Wang et al., 2011) and even more excessive grooming was observed in *Shank3 (13-16)* and *Shank3 (11)* mice (Peça et al., 2011, Schmeisser et al., 2012). No self-grooming was detected in *Shank3 (4-7)* mice and in *Shank3 (9)* mice that showed only a small increase in rearing behavior (Peça et al., 2011, Lee et al.,

2015). These results suggest that different Shank3 isoforms may have different consequences in the expression of the self-grooming phenotype.

Social deficits, which includes a broad range of impairments, such as interaction and communication have been analyzed in Shank3 mutant mice and the results show that all *Shank3* mice, except for *Shank3 (21)*, and *Shank3 (9)* mice, displayed reduced social interaction (Peça et al., 2011, Kouser et al., 2013, Bozdagi et al., 2010, Wang et al., 2011).

ASD is often associated with intellectual disability and, in humans, mutations in *SHANK1-3* genes seems to have a gradient of severity in cognitive impairment (Leblond et al., 2014).

The different *Shank3* mice have different performances in learning and memory tests, suggesting again that each isoform of the protein plays different role in brain functions.

Specifically, *Shank3 (4-9)b* and *Shank3 (21)* were significantly impaired in spatial learning measured by the “water maze test” (Kouser et al., 2013, Wang et al., 2011) instead mild deficits were found in *Shank3 (9)* mice showing only a reduced number of exact platform crossings (Lee et al., 2015) and no defects were detected in *Shank3 (13-16)* and *Shank3 (4-9)b* (Peça et al., 2011, Wang et al., 2011); alterations in short-term and long-term memory were found only in *Shank3 (4-9)b* (Wang et al., 2011).

From the molecular point of view Shank3 mice show a reduction of the glutamatergic synapses and Shank-associated scaffold protein except for *Shank3 (11)* mouse that showed a specific increase of GluN2B in the hippocampus and the *Shank3 (21)* mouse that presents a strong increase of mGlu5 in hippocampal synaptosome preparations (Sala et al., 2015).

Summarizing at the moment we need more detailed studies to correlate phenotypes and molecular diversity in *Shank3* mice.

A simple hypothesis could be that the diversity of phenotypes in *Shank3* mutant mice reflects the molecular diversity of Shank3 protein.

## ***AIM OF THE STUDY***

Shanks/ProSAPs (Shank1, Shank2/ProSAP1 and Shank3/ProSAP2) are a family of scaffold proteins, with a high molecular weight that have a crucial role in organizing the postsynaptic density (PSD) at the excitatory synapses.

All Shanks proteins are characterized by multiple domains: N-terminal ankyrin repeats, an SH3 domain, a PDZ domain, a proline-rich domain, and a sterile alpha motif (SAM) domain. Through these domains Shank proteins interact with a wide variety of different proteins within the PSD including other scaffold proteins, cytoskeletal proteins, signaling molecules and the three major classes of postsynaptic glutamate receptors, guaranteeing proper synaptic formation and function (Uchino and Waga, 2013).

In particular the PDZ domain mediates the binding to AMPA receptors and through SAPAP the binding to PSD-95 and NMDA receptors and the proline rich domain is essential for the binding to Homer, another scaffold protein which binds to metabotropic receptors.

Considering the importance of Shank proteins in proper establishment and maintenance of synaptic contacts and plasticity, is not surprising that mutations in the *SHANK* genes are strongly associated with autism spectrum disorders (ASD) and other neurodevelopmental and neuropsychiatric disorders, such as intellectual disability (ID), and schizophrenia (SCZ) (Grabrucker et al., 2011b).

*SHANK3* was the first gene in the *SHANKs* family reported to be associated with ASDs.

*SHANK3* genetic haploinsufficiency is the major cause of neuropsychiatric symptoms in 22q13.3 deletion syndrome (also known as Phelan-McDermid syndrome, (PMS)) (Uchino and Waga, 2013). Phelan-McDermid syndrome is a complex neurodevelopmental disorder resulting from the loss of the distal long arm of chromosome 22, in particular the q13.3 region. The size of the deleted segments varied widely in individuals with this syndrome, but deletions of *SHANK3* were present in the majority of the cases (Dhar et al., 2010).

PMS is characterized by neonatal hypotonia, global developmental delay, absent or severely delayed speech, autistic-like behaviors and intellectual disability.

The aim of present work was to study the role of Shank3 in synapse formation and function and, in particular, to better understand the involvement of Shank3 on the major neurological features associated with PMS.

In our previous study we used RNAi to knockdown Shank3 expression in neuronal cultures and we demonstrated that the absence of Shank3 causes a reduction of the synaptic expression of metabotropic glutamate receptor 5 (mGlu5), and doesn't affect the expression of other major synaptic proteins.

As a functional consequence of Shank3 knock down we observed an impairment of mGlu5 mediated signaling.

We augmented the activity of mGlu5 using a positive allosteric modulator named 3-Cyano-*N*-(1,3-diphenyl-1*H*-pyrazol-5-yl)benzamide, CDPPB and we found that this treatment was able to rescue, *in vitro*, mGlu5 mediated signaling (Verpelli et al., 2011).

In the present work we analyzed the behavioral phenotypes of *Shank3* $\Delta$ 11<sup>-/-</sup> mice which were generated by deleting exon 11, with the loss of the three major and higher MW isoforms of Shank3 protein.

We found a significant increase of self-grooming activity and a reduction in sociability in KO mice. These data indicate that this mouse model presents repetitive behavior and impaired sociability, the two core symptoms of ASD.

Starting from behavioral data and considering our previous results we decided to investigate the molecular mechanisms underlying the phenotypic deficits, analyzing in particular mGlu5 protein expression and signaling.

We observed that, in striatum and cortex, the absence of Shank3 causes a reduction of mGlu5 and Homer1b/c proteins expression.

Shank3 in these two specific brain regions plays an important role in mediating mGlu5 receptor signaling by recruiting Homer1b/c to the PSD.

We enhanced the activity of mGlu5 receptor with a mGlu positive allosteric modulator, CDPPB and we found that the augmentation of receptor activity ameliorated the behavioral deficits observed in *Shank3* $\Delta$ 11<sup>-/-</sup> mice.

These results provide the rationale to use mGlu5 positive modulators as a possible pharmacological approach to treat patients affected by *SHANK3* mutations and deletions.

## ***MATERIALS AND METHODS***

## DNA CONSTRUCTS AND VECTORS

For plasmid based RNA inhibition, Shank3 and luciferase oligonucleotides were annealed and inserted into the HindIII/BglII sites of the pLVTHM vector for lentivirus production of the shRNA.

It was used the following siRNA sequence, that targets exon 21 of rat and mouse SHANK3 gene (GenBank™ accession number NM\_021676 and NM\_021423.3): 5'-GGAAGTCACCAGAGGACAAGA-3'. The Shank3 rescue (Shank3R) construct, resistant to interference by siRNA, was generated by changing six nucleotides of the siRNA target site, without changing the amino acid sequence of the resultant protein (Verpelli et al., 2011).

## MICE

The *Shank3* $\Delta 11^{-/-}$  mice were kindly provided by Tobias M. Boeckers laboratory from Institute for Anatomy and Cell Biology, Ulm University, Germany as described by Schemeisser et al. 2012 (Schemeisser et al., 2012) and re-derived in a C57BL/6 background (Charles River Laboratories, Calco, Italy). Mice were housed under constant temperature ( $22 \pm 1^\circ\text{C}$ ) and humidity (50%) conditions with a 12 h light/dark cycle, and were provided with food and water ad libitum.

Using heterozygous mice for breeding were obtained wild type and knockout littermates.

All experiments involving animals followed protocols in accordance with the guidelines established by the European Communities Council and the Italian Ministry of Health (Rome, Italy).

## CELL CULTURE PREPARATION AND TRANSFECTION OF PRIMARY RAT AND MOUSE CORTICAL NEURONS

Low density rat cortical neuronal cultures were prepared from 18- to 19-day-old rat embryos as previously described with minor modifications (Verpelli et al., 2011) and were grown in 12-well Petri dishes (Primo).

Mouse cortical neurons were obtained from E18 embryos, grown in 12- or 6-well petri dishes (Primo) and maintained in Neurobasal B27-supplemented medium (Life

Technologies). Rat cortical neurons were transfected using Lipofectamine 2000 on day 11 (DIV11), and the experiments were performed on DIV13-15.

## IMMUNOCYTOCHEMISTRY AND IMAGE ANALYSES

Mouse cortical neurons were fixed at DIV13 in 100% methanol at -20°C for 10 minutes. Rat cortical neurons were transfected at DIV 11 and fixed at DIV15 in 4% paraformaldehyde plus 4% sucrose at room temperature for 5 minutes; then neurons were washed 3 times (10 min for each wash) with PBS (136.8 mM NaCl, 2.68 mM KCl, 10.1 mM Na<sub>2</sub>HPO<sub>4</sub> and 1.76 mM KH<sub>2</sub>PO<sub>4</sub>, pH 7.4 (all Sigma-Aldrich)).

Primary antibodies (anti-Homer1, provided by Enjoom Kim Laboratory, KAIST Institute, Sout Korea and anti-Bassoon, Enzo Life Sciences, cat. ADI-VAM-PS003-F) and secondary antibodies were applied in GDB Buffer in PBS (30 mM phosphate buffer, pH 7.4, 0.2% gelatin, 0.5% Triton X-100, and 0.8 M NaCl).

Mounted coverslips were imaged with a confocal (Zeiss 510 Confocal Microscope, a gift from Fondazione Monzino) with a 63× objective and sequential-acquisition setting at a resolution of 1024 × 1024 pixels. 16 cortical rat transfected neurons for each construct, were chosen randomly for quantification from 4 to 10 coverslips from three independent experiments. A total of 16 neurons (cortical mouse neurons fixed at DIV 15) for each genotype (WT and KO) were randomly chosen for quantification from 4 to 10 coverslips from three independent experiments.

Investigators who were blind to the experimental conditions performed colocalization analyses.

Colocalization measurements were performed using MetaMorph image analysis software (Molecular Devices, Downingtown, PA), by using color-separating Homer and Bassoon channels, manually setting a threshold level for each channel (identical for each neuron), and then determining the overlapping area.

In graph, data are presented as SEM ± standard error.

For the immunodetection of postsynaptic density markers on brain sections, the mice were anesthetized intraperitoneally using Avertin (Sigma-Aldrich) and then decapitated. The brains were rapidly excised and manually cut into coronal slabs that were fixed via immersion in ice-cold paraformaldehyde (4% in 0.1 M phosphate buffer, PB, pH 7.4) for 30 min (Giustetto et al., 1998). After fixation, the tissue slabs were rinsed in PBS, cryoprotected via immersion in ascending sucrose solutions

(10%, 20% and 30%), cut into 20- $\mu$ m sections with a cryostat, mounted on gelatin-coated slides and stored for a maximum of one month at  $-20^{\circ}\text{C}$  until immunolabeling was performed. Following blocking in normal donkey serum (NDS, 3% in PBS with 0.5% Triton X-100), the sections were incubated with primary antibodies diluted in PBS containing 3% NGS and 0.5% Triton X-100 overnight at  $4^{\circ}\text{C}$  (anti-PSD-95 NeuroMab, Ca, USA cat. 75-028 and anti-Homer1 provided by Enjoom Kim Laboratory, KAIST Institute, Sout Korea). The sections were then washed and incubated with secondary antibodies that were diluted in 3% NGS and 0.5% Triton X-100 in PBS for 1 hour at room temperature. The sections were rinsed again and coverslipped with Dako fluorescence mounting medium (Dako Italia, Italy). For quantitative analysis of Homer1-immunoreactive puncta and colocalization studies, 5 serial optical sections (using a 0.5- $\mu$ m Z-step size) were acquired from sections including layers 2-3 of the primary somatosensory cortex (S1), the CA1 region of the hippocampus (stratum radiatum) and the dorsal striatum (caudate and putamen nuclei) using a laser scanning confocal microscope (LSM5 Pascal; Zeiss) with a 100 $\times$  objective (1.4 numerical aperture) and the pinhole set at 1 Airy unit. The density of the immunolabeled puncta was determined by manually counting postsynaptic clusters in neuropilar areas using dedicated software (Imaris, Bitplane, Zurich, CH) and expressed as puncta/100  $\mu\text{m}^2$ .

## SUBCELLULAR FRACTIONATION AND WESTERN BLOT ANALYSIS

Subcellular fractionation of mice brain tissues was performed according to *Distler et al.* (*Distler et al., 2014*) with some modifications.

Tissues were homogenized in buffer A containing 0.32 M sucrose and 5 mM HEPES (pH7.4) and centrifuged at 1.000 x g. The supernatant (S1) was further centrifuged at 12.000 x g, and a pellet containing the crude membrane fraction (P2) was obtained. This fraction was solubilized in buffer B containing 0.32 M sucrose and 5 mM Tris (pH 8.1) and loaded onto a discontinuous sucrose step gradient (0.85 M/1.0 M/1.2 M). After centrifugation at 85.000 x g, the synaptosomes were collected from the 1.0 M/1.2 M interface and incubated with buffer C containing 0.32 M sucrose, 12 mM Tris (pH 8.1) and 1% Triton X-100. After centrifugation at 32.800 x g, the PSD pellet was collected and solubilized in  $\text{H}_2\text{O}$ .

After protein extraction, 10 ug of each sample were electrophoretically separated using SDS-PAGE and then blotted on nitrocellulose membranes according to standard protocols.

Incubation with a primary antibody ( $\beta$ -actin Sigma, cat. A5316; Homer1b/c, SynapticSystems, cat. 160022,; mGluR5, Millipore, cat. AB5675; Shank3, Santa Cruz Biothecnology, cat. H-160;  $\beta$ 3-tubulin, Covance, cat. PRB-435P) was followed by treatment of the membrane with HRP-conjugated secondary antibodies, and the signal was visualized using Pierce ECL Western Blotting Substrate and further detected using a MicroChemi 4.2 machine. All signals were quantified using Gel analyzer software ([www.gelanalyzer.com/](http://www.gelanalyzer.com/)) and normalized against the values of the respective signal for  $\beta$ -actin or PSD-95.

## IMMUNOPRECIPITATION ASSAY

PSD-enriched preparations (as described above) of different brain regions (cortex, hippocampus and striatum) from P60 WT and KO mice were incubated at 4°C overnight with protein A-Sepharose beads conjugated to rabbit Homer1b/c (10  $\mu$ g/ml Santa Cruz cat. H-342) antibody and relative control IgG (10  $\mu$ g/ml). The beads were then washed three times with Buffer C, re-suspended in sample buffer, warmed at 65°C for 10 minutes and analyzed using SDS-PAGE. Western blot analysis was performed using mGlu5 (Millipore, cat. AB5675) primary antibody.

## FURA-2 SINGLE CELL Ca<sup>2+</sup> IMAGING

All measurements were carried out thanks to the collaboration with Department of Pharmaceutical Sciences, University of Eastern Piedmont “Amedeo Avogadro” (Novara, Italy) and analyses were kindly performed by Dr. Dmitry Lim.

For Ca<sup>2+</sup> measurements, 0.3 mln neurons were plated onto 24-mm round coverslips in 6-well plates. At DIV12-DIV14, the plates were loaded with 5  $\mu$ M Fura-2 AM (Life Technologies, Milan, Italy) containing 0.002% Pluronic F-127 (Life Technologies) and 10  $\mu$ M sulfinpyrazone (Sigma) in Krebs-Ringer modified buffer (KRB solution: 125 mM NaCl, 5 mM KCl, 1 mM Na<sub>3</sub>PO<sub>4</sub>, 1 mM MgSO<sub>4</sub>, 2 mM CaCl<sub>2</sub> 5.5 mM glucose, and 20 mM HEPES, pH 7.4) for 30 min at room temperature (RT). The neurons were then washed twice in KRB, and the Fura-2 was allowed to de-esterify

for another 30 min at RT. The coverslips were then mounted in the acquisition chamber of a Leica DMI6000 epifluorescent microscope equipped with an S Fluor 40x/1.3 objective. First, neurons expressing a GFP-tagged shShank3 or control (shCtrl) plasmid were imaged and photographed using Leica AM Meta Morph software (Molecular Devices, Sunnyvale, CA, US) at an excitation wavelength of 488 with a bandpass 510-nm emission filter. The cells were then alternately excited at 340 and 380 nm using a monochromator Policrome V (Till Photonics, Munich, Germany), and images of the fluorescent signals were captured each second through bandpass 510 nm filter using a CCD camera (Hamamatsu, Japan). All hardware was controlled, and Fura-2 images were analyzed using MetaFluor (Molecular Devices) software. To quantify differences in the amplitudes of  $\text{Ca}^{2+}$  transients, the ratio values were normalized using the formula  $(DF)/F_0$  (referred to as norm. ratio). To compare multiple samples (e.g., shShank3 and rescue results), ANOVA was used with Tukey's post-hoc tests. To analyze differences between two samples (e.g., Shank3-KO results) Student's two-tailed unpaired t-tests were used. Differences were considered statistically significant when  $p < 0.05$ .

## ELECTROPHYSIOLOGY

All the experiments were carried out thanks to the collaboration with the University of Perugia and analyses were performed by Paolo Calabresi laboratory.

Mice were sacrificed by cervical dislocation and coronal corticostriatal slices (250  $\mu\text{m}$ ) were cut in Krebs' solution (in mM: 126 NaCl, 2.5 KCl, 1.2  $\text{MgCl}_2$ , 1.2  $\text{NaH}_2\text{PO}_4$ , 2.4  $\text{CaCl}_2$ , 10 glucose, 25  $\text{NaHCO}_3$ ) using a vibratome. The slices were maintained in Krebs' solution, bubbled with a  $\text{O}_2$  95% and  $\text{CO}_2$  5% gas mixture at room temperature (Calabresi et al., 1992). A single slice was transferred to a recording chamber and submerged in a continuously flowing Krebs' solution ( $34^\circ\text{C}$ , 2.5–3 ml/min) bubbled with a 95 %  $\text{O}_2$ –5 %  $\text{CO}_2$  gas mixture. Whole-cell patch-clamp recordings were obtained from dorsolateral striatal neurons optically detected (Olympus) and electrophysiologically identified as MSNs (Calabresi et al., 1992). Whole-cell voltage-clamp ( $V_{\text{hold}} -80$  mV) or current-clamp recordings were performed with borosilicate glass pipettes (4–7  $\text{M}\Omega$ ;  $R_a$  15–30  $\text{M}\Omega$ ) filled with a standard internal solution containing (in mM): 125  $\text{K}^+$ -gluconate, 0.1  $\text{CaCl}_2$ , 2  $\text{MgCl}_2$ , 0.1 EGTA, 10 HEPES, adjusted to pH 7.3 with KOH. Signals were amplified with a

Multiclamp 700B amplifier (Molecular Devices), recorded and stored on PC using pClamp 10 (Molecular Devices). Membrane potentials and currents were recorded in the presence of 50  $\mu$ M picrotoxin to block GABA<sub>A</sub> receptors. Glutamatergic excitatory postsynaptic currents (EPSCs) were evoked by a bipolar electrode connected to a stimulation unit (Grass Telefactor) and located in the white matter between the cortex and the striatum. Paired-pulse ratios of EPSC amplitudes (EPSC2/EPSC1) were obtained by a paired-pulse stimulation protocol at 50 ms inter-stimulus interval.

Drugs were bath-applied by switching the perfusion solution to drug-containing solution using a three-way tap syringe. Total replacement of the medium in the chamber occurred within 1 minute. CDPPB, CHPG, DHPG, NMDA, muscarine, picrotoxin, L-SOP, were purchased from Tocris-Cookson (Bristol, UK). CHPG, DHPG and muscarine were bath applied in the recording chamber alone and then co-applied with NMDA.

Data analysis was performed off-line using Clampfit 10 (Molecular Devices) and GraphPad Prism 5 (GraphPad Software). Values in the text and figures are mean  $\pm$  S.E., n representing the number of recorded neurons. Student's *t*-test was used for statistical analysis with a significance level established at  $P < 0.05$ .

## BEHAVIORAL ASSAYS

For behavioral analyses, 3-month-old age-matched littermate mice were used. All tests were performed between 8 a.m. and 2 p.m.

### *-Spontaneous motor activity*

Motor function was evaluated in an activity cage (43  $\times$  43  $\times$  32 cm) (Ugo Basile, Varese, Italy) that was placed in a sound-attenuating room as previously described (Sala et al., 2011). The cage was fitted with two horizontal and vertical infrared beams that were located 2 cm and 4 cm from the floor of the cage, respectively. Before the test each mouse was put in the testing room for 1 h. Cumulative horizontal and vertical movement counts were recorded for 10 min.

### *-Repetitive self-grooming*

Spontaneous repetitive self-grooming behavior was scored as previously described (McFarlane et al., 2008). Each mouse was placed into a standard cylinder, (46 cm length × 23.5 cm wide × 20 cm high).

After a 10-min habituation period in the test cage, each mouse was scored with a 10 min stopwatch for cumulative time spent grooming all body regions. The observer stayed at a distance of approximately 2 m from the test cage, and was blind to genotype while scoring self-grooming.

### *-Spatial object recognition*

Object location tests were carried out in an arena according to Kenney et al. (Kenney et al., 2011), with minor modifications. Two visual cues were placed on two adjacent walls of an opaque white Plexiglas cage (58×50×43 cm) that was dimly lit from above (27 lux). The visual cues consisted of a black and white striped pattern (21×19.5 cm) that was affixed to the center of the northern wall and a black and gray checkered pattern (26.5×20 cm) that was placed in the center of the western wall. The objects were counterbalanced across locations. The cage and the objects were thoroughly wiped down with acetic acid (0.1%) before and after all behavioral procedures, which were observed and recorded using a camera mounted above the cage. Climbing or sitting on objects was not scored as object exploration. Mice that did not spend more than a total of 30 s exploring the objects during training or testing were excluded from the analysis. Mice were pre-exposed to the cage for 10 min. Twenty-four hours later, the mice were returned to the cage and allowed to explore two different objects placed in the NE and NW corners, and the time spent exploring the objects was recorded. Two hours later, the object the mouse had spent more time exploring in the previous session was moved to the SW corner of the cage (only this object was placed in the cage), and the mouse was allowed to re-explore the cage. Exploration was defined as a mouse having its nose directed toward the object and within approximately 1 cm of the object (Bevins and Besheer, 2006). Performance was evaluated by calculating a discrimination index  $(N-F/N+F)$ , where N = the time spent exploring the moved object during  $T_2$ , and F = the time spent exploring the stationary object during  $T_2$ .

### *-Sociability and Preference for Social Novelty Tests*

The apparatus was a rectangular, three-chamber, transparent polycarbonate box (width = 42.5 cm, height = 22.2 cm, center chamber length = 17.8 cm, and side

chamber lengths = 19.1 cm) as previously described <sup>27</sup>. The test mouse was first placed in the middle compartment, and it was allowed to explore all three chambers for 10 min (habituation). Then, an unfamiliar adult DBA/2J male mouse was placed in one side compartment. The opposite side compartment contained an empty wire cage. The social novelty tests were performed in the same apparatus immediately after sociability test. The cages were not cleaned between these two tests. For these tests, one side compartment contained the familiar mouse (from the previous sociability phase), while the other side contained an unfamiliar mouse. The new, unfamiliar mouse was placed in the wire cage that had been empty during the prior 10-min session. The familiar and unfamiliar animals were from different home cages and had never been in physical contact with the subject mouse or with each other. For both tests, the time spent in each chamber and the number of entries into each chamber were recorded for 10 min. The data were expressed as the difference in the scores between the time spent exploring the compartment containing the familiar mouse and the time spent in the empty compartment (for sociability tests) or the difference in the scores between the time spent containing the stranger animal and the time spent with the familiar mouse (for social novelty tests). An operator blind to the genotypes of the mice manually recorded the time spent in each chamber. We also evaluated a sociability index (SI) and a social novelty preference index (SNI) as follows:  $SI = (\text{time exploring novel mouse 1} - \text{time exploring novel object}) / (\text{time exploring novel mouse 1} + \text{time exploring novel object})$  and  $SNI = (\text{time exploring novel mouse 2} - \text{time exploring familiar mouse}) / (\text{time exploring novel mouse 2} + \text{time exploring familiar mouse})$ .

#### *-Morris water maze test*

The Morris water maze test was adapted from mice and used to analyze changes in the learning and memory abilities of the mice according to the methods described in Morris (Morris, 1984). A circular water maze (120 cm in diameter x 50 cm in height) was used. A circular hidden platform with a diameter of 10 cm was placed inside the maze, and its surface was maintained at 0.5 cm below the surface of the water. Floating plastic particles were placed on the surface of the water to hide the platform from sight according to the methods of Zhang (Zhang et al., 2013). The temperature of the water was  $25.0^{\circ}\text{C} \pm 0.5^{\circ}\text{C}$ . For the habituation trials, the mice were placed in a random area inside the maze and allowed to swim for 60 sec. For the acquisition trials, the mice were submitted to 4 trials per day (with 60 sec inter-trial intervals) for

4 consecutive days during which each mouse was released into the pool at different starting points and trained to locate a constant platform position. At 24 hours after the last trial, a probe test was performed during which the platform was removed. Two days later, a reversal task was performed to assess cognitive flexibility. The platform was placed in the opposite quadrant of the tank, and 4 daily trials were performed for 4 days. On the fifth day, a probe trial was performed that was similar to that in the acquisition phase. The time spent in the target area and the latency to reaching the target zone were evaluated by an experimenter who was blind to the genotypes of the mice. After each trial, the mice were placed on a paper towel to dry, and they were then placed back into their home cages.

#### *-T-maze test*

Mice were deprived of food until they reached 85–90% of their free-feeding body weight. They were habituated to a black wooden T-maze (with a 41-cm stem section and a 91-cm arms section). Each section was 11 cm wide and had walls that were 19 cm high. The mice were habituated to the T-maze and trained to obtain food within the maze for 5 days as previously described (Sala et al., 2011). During the acquisition phase, one arm was designated the reinforcer (Coco Pops; Kellogg's) in each of ten daily trials. Each mouse was placed at the start of the maze and allowed to freely choose which arm to enter. The number of days required to reach the goal criterion (80% correct for 3 days) was recorded. Each mouse that met the goal for acquisition was then tested using a reversal procedure in which the reinforcer was switched to the opposite arm.

## PHARMACOLOGICAL TREATMENTS

CDPPB (Tocris) was resuspended in DMSO and polyethylene glycol 400 (DMSO:PEG 400 = 1:9). 70 min before each behavioral test. Wild-type and *Shank3 $\Delta$ 11*<sup>-/-</sup> mice were injected intraperitoneally with CDPPB (3 mg/kg) containing solution or the same volume of a DMSO:PEG400 mixture.

## iPSC GENERATION AND DIFFERENTIATION INTO NEURONS

Patients diagnosed with Phelan-McDermid syndrome, using genetic analysis, were involved in this study.

Fibroblast from patients and healthy donors were collected according to a clinical protocol approved by the local Bioethical Committees of different medical centers. All the individuals involved in the study were informed of the objectives of the study and were required to sign an informed consent document before inclusion into the study. The generation, maintaining and characterization of iPS cells were performed as described by Verpelli et al, 2013 (Verpelli et al., 2013). These primary antibodies were used for immunofluorescence analysis on iPS cells and differentiated neurons: Nanog (Abcam cat. AB80892), Oct3/4 (Santa Cruz Biotechnology cat. sc-5279), Sox2 (Proteintech cat. 11064-1-AP), MAP2 (Abcam cat. AB11268), Synaptophysin (Sigma MS5768).

## STATISTICS

All quantitative biochemical data are representative of three independent experiments, and all behavioral data are representative of at least two experiments. Unpaired two-tailed *t*-test was used to evaluate the difference between two groups. The variances in two groups were similar in all data sets. Two-way analysis of variance followed by *post hoc* test was used for comparison of multiple samples. Significance was set at  $P < 0.05$ . All values are presented as mean  $\pm$  SEM.

# ***RESULTS***

## Deletion of Exon 11 of *SHANK3* gene causes ASD-like behaviors in mice

To clarify if a *SHANK3* mutation in mice causes ASD-like behaviors and intellectual disability we characterized the behavior of *Shank3 $\Delta$ 11<sup>-/-</sup>* mice, previously generated deleting the exon 11 of the *SHANK3* gene (Schmeisser et al., 2012).

ASD includes various neurodevelopmental disorders, characterized by two behavioral domains: repetitive/stereotypic behaviors and impaired social interaction. All the behavioral experiments were performed in collaboration with Prof. Maria Elvina Sala.

As a measure of repetitive behavior we analyzed grooming behavior; *Shank3 $\Delta$ 11<sup>-/-</sup>* mice present an increased self-grooming activity in terms of time spent grooming and number of grooming episodes (**Figure 1A**).

The second core symptom of ASD is the impairment of social interaction; for this reason we tested *Shank3 $\Delta$ 11<sup>-/-</sup>* mice for sociability using the three chambers test (**Figure 1B**).

KO mice spent more time exploring the compartment with the empty cage than the one with the stranger mouse (**Figure 1B left**) and remained closer to the family stranger for longer time, suggesting an impairment in sociability and social recognition (**Figure 1B right**).

Accordingly, the corresponding sociability index (SI) and social novelty preference index (SNI) scores were lower in KO mice than their WT littermates.

Mutations in *SHANK3* gene are associated with intellectual disability, for this reason we tested spatial learning and memory of KO mice.

To evaluate spatial memory, we used a spatial object recognition test in which we analyzed a discrimination index with an inter-trial interval of 120 min. We did not detect significant differences between WT and KO mice (**Figure 1C**).

We also tested mice with Morris Water maze test and we found that KO mice showed normal acquisition compared to WT littermates (**Figure 1D left**). Spatial memory was then tested using a probe trial, which was administered after a 4-day training period during which we measured the latency (**Figure 1D, center**) and the time required to reach the target quadrant (**Figure 1D, right**). We did not detect any significant difference between the genotypes. The latency and the percentage of time spent swimming to the target quadrant were also not significantly different. On

the contrary, the escape latency of KO mice was longer than the latency in WT mice on day 8 and day 9 (**Figure 1E, left**). In the probe trial, the KO mice took longer to find the target zone (**Figure 1E, center**) and spent less time than WT mice to swim to the quadrant that previously housed the platform (**Figure 1E, right**).

Shank3 $\Delta$ 11<sup>-/-</sup> mice also showed impairments in the T-maze task, but only during the reversal phase (**Figure 1F**). KO mice required more days to achieve the criterion than WT mice. These results indicate that KO mice show a resistance in changing a learned pattern of behaviors, suggesting a cognitive rigidity.

Taken together our behavioral data demonstrate that *Shank3* $\Delta$ 11<sup>-/-</sup> is a good mouse model to clarify the role of Shank3 in PMS because this mutant line shows the main behavioral features associated to PMS.

### **Shank3 absence alters Homer and mGlu5 synaptic localization**

Shank3 is a multidomain protein localized at the PSD of glutamatergic synapses where it acts as a major scaffold protein interacting directly or indirectly with all types of glutamate receptors and cytoskeletal elements via different domains.

In particular the association between Shank3 and type I of metabotropic receptors, which includes mGlu5, is ensured by the interaction between Homer1 and the proline rich domain of Shank3.

In our previous work we demonstrated that knock-down of Shank3, using a shRNA technique, in primary neurons causes a significant reduction of mGlu5 protein expression (Verpelli et al., 2011).

Based on these results we decided to measure mGlu5 and Homer1b/c protein levels in the PSD fraction of striatum, cortex and hippocampus of *Shank3* $\Delta$ 11<sup>-/-</sup> mice (**Figure 2A**). We found a reduction of Homer1b/c protein levels in striatum (**Figure 2A left**), a reduction of both mGlu5 and Homer1b/c in cortex (**Figure 2A center**) and non change in mGlu5 and Homer1b/c in hippocampus (**Figure 2A right**).

This biochemical analysis indicates that the absence of Shank3 alters, in vivo, mGlu5 and Homer1b/c protein expression specifically in the PSD of two brain regions, cortex and striatum.

To understand whether the localization of Homer was altered in absence of Shank3, we next analyzed postsynaptic Homer1 localization in the dorsal striatum, in layers

2-3 of the primary somatosensory cortex and in the CA1 stratum radiatum of the hippocampus in *Shank3 $\Delta$ 11*<sup>-/-</sup> mice using immunofluorescence and confocal microscopy (**Figure 2B**).

From this analysis we found that the total density of Homer1-positive puncta is unchanged between WT and KO mice in all the brain regions (**Figure 2B**).

KO mice showed an increase of Homer1 puncta not colocalizing with PSD-95 and in parallel, a significant reduction of double-labeled puncta both in dorsal striatum and in somatosensory cortex (**Figure 2B**). We did not observe any changes in Homer1 localization in the CA1 area of hippocampus in this analysis too (**Figure 2B**).

To understand if this alteration in the synaptic localization of Homer1 causes a reduction of the interaction between Homer and mGlu5 we co-immunoprecipitated both proteins in striatum, cortex and hippocampus of WT and KO mice (**Figure 2C**).

Western blot analysis revealed a significant reduction of mGlu5 and Homer1b/c protein-protein interaction in both striatum and cortex but not in hippocampus of *Shank3 $\Delta$ 11*<sup>-/-</sup> mice compared to WT littermates (**Figure 2C**).

From our biochemical and immunohistochemical studies we can conclude that the absence of Shank3 causes brain-specific alteration of both protein expression and localization of mGlu5 and Homer1b/c at synapses, preventing in this way the correct formation of mGlu5/Homer complex, which is essential to mediate mGlu5 intracellular signaling.

### **Shank3 absence impairs mGlu5-mediated intracellular calcium release**

mGlu5 receptor is a metabotropic receptor coupled to Gq/G11 G-protein. The stimulation of the receptor causes the activation of phospholipase C (PLC), a Ca<sup>2+</sup>-dependent enzyme that catalyzes the hydrolysis of phosphatidylinositol 4,5 bisphosphate (PIP<sub>2</sub>) to yield inositol 1,4,5 trisphosphate (IP<sub>3</sub>) and diacylglycerol (DAG), which are important cellular second messengers. In particular IP<sub>3</sub>, binding to IP<sub>3</sub> receptors, causes an increase of calcium release from intracellular stores resulting in cell depolarization, enhanced cell excitability, and activation of numerous intracellular signaling molecules such as protein kinase A (PKA), protein kinase C (PKC), mitogen-activated protein kinase (MAPK), extracellular signal related kinase

(ERK), and cAMP response element binding protein (CREB) (Cleva and Olive, 2011).

Interestingly Homer protein, thanks to its EVH1 domain, is able to bind both mGlu5 receptor and the inositol tri-phosphate (IP3) receptors. Thus Homer physically and functionally links mGlu5 receptors to their downstream effectors, the IP3 receptors, allowing a more efficient release of intracellular calcium in response to receptor stimulation (Sheng and Kim, 2000).

Considering that we found alterations in Homer and mGlu5 synaptic expression, interaction and localization in *Shank3 $\Delta$ 11<sup>-/-</sup>* mice, we investigated if the absence of Shank3 altered the generation of mGlu5-mediated Ca<sup>2+</sup> signals, using cortical neurons obtained from *Shank3 $\Delta$ 11<sup>-/-</sup>* mice.

First, we confirmed that the reduction of the mGlu5 receptor and Homer1b/c protein levels that was observed in the cortex was also observed in the synaptic fractions of cultured cortical neurons obtained from *Shank3 $\Delta$ 11<sup>-/-</sup>* mice (**Figure 3A**). Then, we measured the induction of Ca<sup>2+</sup> transients by 200  $\mu$ M DHPG ((S)-3,5-Dihydroxyphenylglycine), a specific group I metabotropic receptor agonist. **Figure 3B** shows that DHPG-induced Ca<sup>2+</sup> transients in KO neurons were significantly lower than in WT neurons, indicating that the absence of the Shank3 protein impaired mGlu5-mediated signaling in cortical neurons.

To confirm that these alterations in calcium signaling mediated by mGlu5 receptor activation were due to alterations in the synaptic localization of Homer, we analyzed the synaptic distribution of Homer1b/c using immunofluorescence in cultured cortical neurons that were derived from *Shank3 $\Delta$ 11<sup>-/-</sup>* and WT mice. Quantification of the co-localization of Homer puncta and Bassoon (a presynaptic marker) revealed that the postsynaptic localization of Homer was reduced in the *Shank3 $\Delta$ 11<sup>-/-</sup>* cortical cultured neurons (**Figure 3C**).

Verpelli et al. (Verpelli et al., 2011) previously demonstrated that *in vitro*, the reduction of mGlu5 receptor activity that was caused by Shank3 knock-down could be rescued using an allosteric mGlu5 positive modulator CDPBB.

For this reason we tried to rescue deficits in mGlu5-mediated Ca<sup>2+</sup> signals using CDPBB in cortical neurons obtained from KO mice.

In these experiments, DIV12-14 cortical neuronal cultures were loaded with Fura-2 and challenged with 200  $\mu$ M DHPG in either the presence (5 min of preincubation) or the absence of 3  $\mu$ M CDPBB (**Figure 3D**). As expected, in the *Shank3 $\Delta$ 11<sup>-/-</sup>*

cortical neurons, the DHPG-induced  $\text{Ca}^{2+}$  transients were approximately 40% lower than in the WT neurons. After preincubation with CDPPB, the  $\text{Ca}^{2+}$  transients in the *Shank3 $\Delta$ 11<sup>-/-</sup>* neurons were significantly augmented, reaching the level of WT neurons (**Figure 3D**).

In addition to these we performed other experiments, in which we knocked down Shank3 using specific shRNA sequences.

**Figures 3E and G** show that the administration of 200  $\mu\text{M}$  DHPG elicited a much lower  $\text{Ca}^{2+}$  transient in shRNA-Shank3-transfected neurons than in control neurons (either non-transfected or transfected with a GFP-expressing plasmid). When the shShank3-resistant form of Shank3 was co-expressed with the shRNA-Shank3 plasmid, the DHPG-induced  $\text{Ca}^{2+}$  transients were restored to control levels, indicating that the effect of shRNA-Shank3 transfection was specific. We confirmed using immunofluorescence that Homer-Bassoon co-localization was altered also in Shank3 knock-down neurons (**Figure 3F**).

These sets of experiments demonstrates that the absence of Shank3, *in vitro*, causes an impairment of mGlu5-mediated  $\text{Ca}^{2+}$  release that can be restored by the application of CDPPB, a positive mGlu5 receptor allosteric modulator.

### **The effect of mGlu5 stimulation on NMDA responses in striatal medium spiny neurons is dependent on Shank3**

Because we observed, in striatum, a disruption in synaptic Homer localization in the absence of Shank3, we tested the electrophysiological properties of striatal neurons. Patch-clamp recordings were measured using medium spiny neurons (MSNs) obtained from WT and KO mice to explore whether the deletion of Shank3 affected the basal membrane properties of striatal neurons. Current-voltage curves were obtained by delivering hyperpolarizing and depolarizing steps of currents to the MSNs of KO (n=6) and WT (n=6) mice, and we observed no difference between these two groups of neurons, suggesting that the basal membrane properties of MSNs do not depend on Shank3 expression (**Figure 4A-B**).

We subsequently studied whether Shank3 was responsible for the observed changes in the membrane potential and the ionic currents induced by the stimulation of group I mGlu receptors in MSNs. Activation of these types of metabotropic

glutamate receptors has been shown to enhance the membrane depolarization/inward current that is produced by the activation of the NMDA receptor in striatal MSNs (Pisani et al., 2001). As shown in **Figures 4C and 4G**, the application of 30  $\mu$ M NMDA produced a membrane depolarization of approximately 15 mV and an inward current of approximately -70 pA in MSNs in WT mice, while the co-application of NMDA in the presence of DHPG produced a significantly larger depolarization (**Figure 4C-D**) and inward current (**Figure 4 G-H**). Interestingly, in the MSNs obtained from KO mice, the co-application of NMDA and DHPG failed to produce a membrane depolarization and inward current that was larger than those observed in the presence of NMDA alone (**Fig. 4E-H**).

We then tested the effect of CDPPB on MSNs obtained from WT and KO mice, and as shown in **Figures 4I-J**, CDPPB treatment was able to recover normal NMDA receptor functions, which depend on mGlu5 receptor activity, in the MSNs obtained from Shank3 KO mice to levels comparable to those in the MSNs obtained from WT mice.

### **CDPPB is able to rescue ASD-like behaviors in *Shank3 $\Delta$ 11*<sup>-/-</sup> mice**

In our previous work we demonstrated that, *in vitro*, the treatment with CDPPB is able to restore mGlu5 reduced activity due to the knocking down of Shank3 (Verpelli et al., 2011). In addition, from calcium imaging analysis performed on neurons obtained from KO mice we found that CDPPB treatment rescues the Ca<sup>2+</sup> transients to WT levels (**Figure 3D**). Further to these results we found that CDPPB treatment is able to recover normal NMDA receptor functions, which depend on mGlu5 receptor activity, in the MSNs of Shank3 mutant mice.

Thus, we decided to test if behavioral deficits found in *Shank3 $\Delta$ 11*<sup>-/-</sup> mice could be pharmacologically ameliorated treating KO mice with CDPPB.

We evaluated the behavioral phenotypes of KO mice after treatment with CDPPB (3mg/kg i.p.) or vehicle (veh), which were administered acutely or repeatedly 70 min before each test.

The treatment with CDPPB doesn't affect the mice motor activity (**Figure5A**).

Acute CDPPB treatment causes a reduction of grooming time and grooming episodes in KO mice compared to the same genotype treated with vehicle (**Figure 5B**).

Reduced sociability (**Figure 5C, left**) was slightly, but not significantly, rescued in KO animals by acute treatment with CDPPB when analyzed as time spent close to the stranger/object. However, the SI, which measures sniffing activity, was significantly increased when the animals received CDPPB. Social recognition was completely rescued in *Shank3Δ11*<sup>-/-</sup> mice, when analyzed as either the time spent close to the stranger2/stranger1 or sniffing activity (**Figure 5C, right**).

In the water-maze place navigation task (**Figure 5D**), the KO mice showed normal acquisition compared to WT mice in terms of mean time required to reach the platform. A significant latency reduction between the first and the fourth trial was observed in all groups (**Figure 5D, left**), suggesting a normal progression of learning. During the probe test, no difference among the groups was shown in latency (**Figure 5D, center**) or the time spent in the target zone (**Figure 5D, right**). During reversal (**Figure 5E**), a significant difference in the escape latency across the trials was observed. KO mice treated with vehicle were completely impaired compared to their littermates, while CDPPB reduced escape latency during the learning phase (**Figure 5E, left**).

When submitted to the probe trial on day 10, KO mice that were treated with CDPPB required less time to find the target zone (**Figure 5E, center**) and spent more time than the KO mice treated with vehicle to swim to the quadrant that previously housed the platform (**Figure 5E, right**).

These pharmacological data suggest that positive allosteric modulation of mGlu5 receptors, using CDPPB, is able to rescue the ASD-like behaviors, due to altered mGlu5 signaling, found in *Shank3Δ11*<sup>-/-</sup> mice.

### **Shank3 absence causes alterations of Homer localization in neurons derived from patients affected by Phelan McDermid Syndrome (PMS)**

Considering the limitations of mouse models and the great heterogeneity of patients with PMS, in terms of clinical features and size of deletions, another important model to study the PMS is represented by induced pluripotent stem cells (iPSCs).

Indeed many limitations of mouse models can be overcome with the use of iPSC technology, which allows the generation of personalized human neurons from patients.

Donor-derived cells (e.g., dermal fibroblasts from a skin biopsy) were reprogrammed into iPSCs by forced expression of four pluripotency-associated transcription factors: OCT4, SOX2, KLF4, and c-MYC.

In particular we established iPSC lines from two different patients with PMS, one with a deletion of approximately 7.99Mb (named Patient 1) and one with a deletion 22q13.3 ARSA negative (named Patient 2). As control we used iPSCs obtained from two healthy donors.

All iPSC clones were analyzed by immunofluorescence (**Figure 6A**) and PCR (**Figure 6B**) to test the expression of endogenous pluripotency markers.

iPSC clones were then differentiated into cortical neurons via the generation of neural-rosette intermediate neural progenitors, and they were subsequently differentiated for 80 days. We confirmed using WB that there was a reduction in Shank3 protein levels in the neurons obtained from both of the PMS patients compared to the Shank3 levels in the controls (**Figure 6C**). To analyze Homer cluster localization, we infected neuronal progenitors with a lentivirus expressing Homer-GFP. Interestingly, after 80 days of differentiation, we observed a significant reduction in the number of Homer puncta that co-localized with Synaptophysin in neurons derived from both of the PMS patients compared to the co-localization observed in neurons derived from the controls (**Figure 6D**).

These data confirm that also in human neurons, derived from patients affected by PMS, the absence of Shank3 causes an alteration of Homer1b/c synaptic localization.

# ***FIGURES***

Figure 1

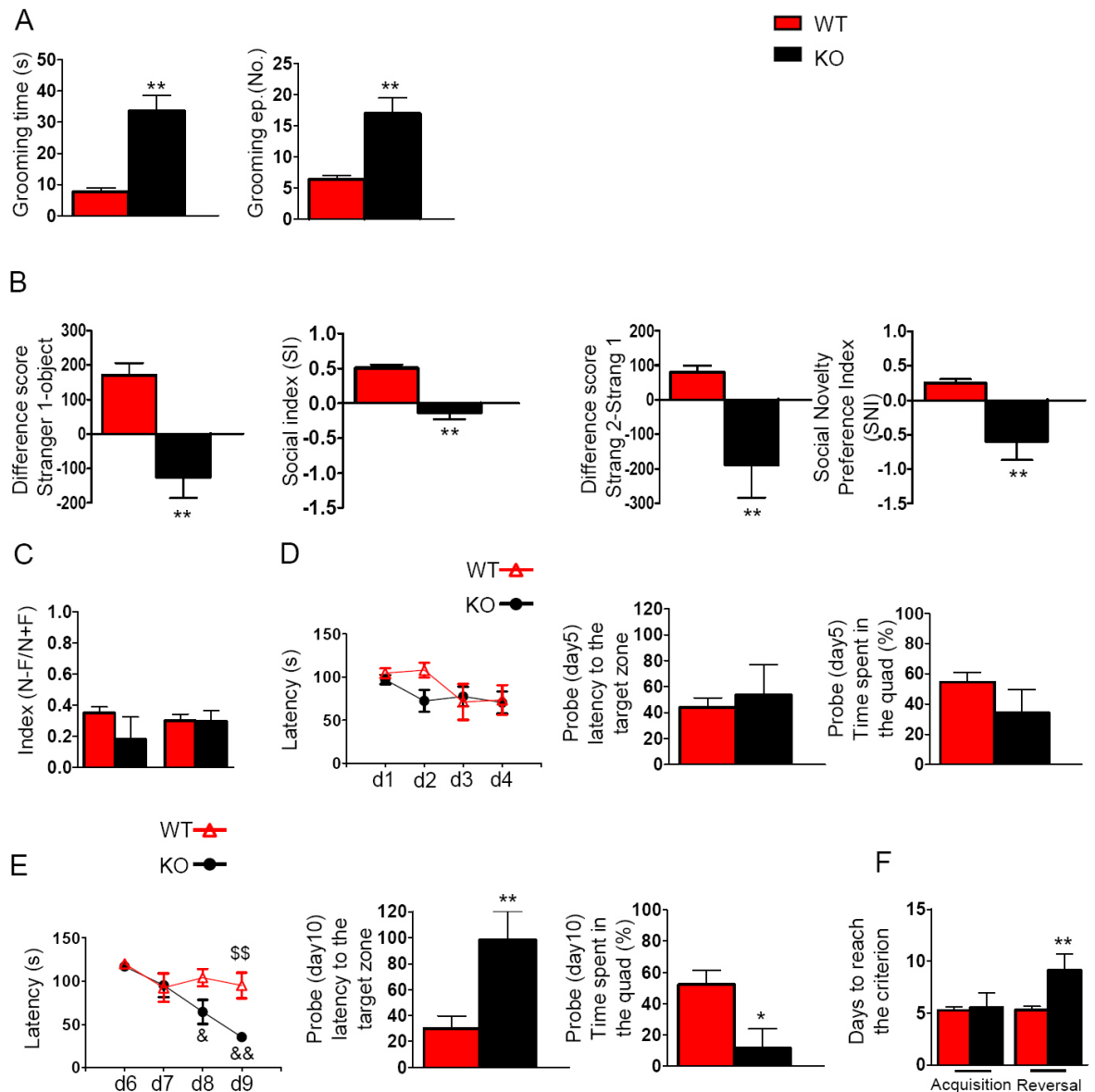


**Figure 1: Deletion of Exon 11 of *SHANK3* gene causes ASD-like behaviors in mice**

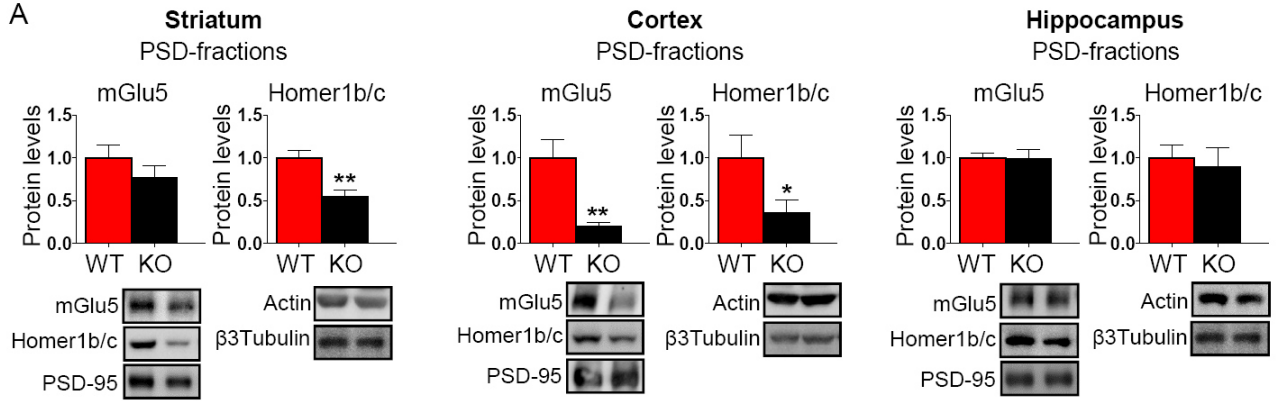
**A)** Self-grooming behavior was evaluated as the time spent grooming (left) and the total number of grooming episodes (right). **B)** Differences in scores obtained for time spent in the chamber associated with the never seen before mouse and the empty cage (left) or the familiar mouse (preference for social novelty test) (right). **C)** Spatial memory was evaluated by determining a discrimination index in the spatial object recognition test. **D-E)** Acquisition and reversal in the Morris water maze was analyzed to determine learning patterns (left), escape latency to the target zone

(center) and the time spent in the quadrant (right). **F**) Performance in the T maze test was analyzed as the number of days required to reach the criterion during the acquisition and reversal phases.

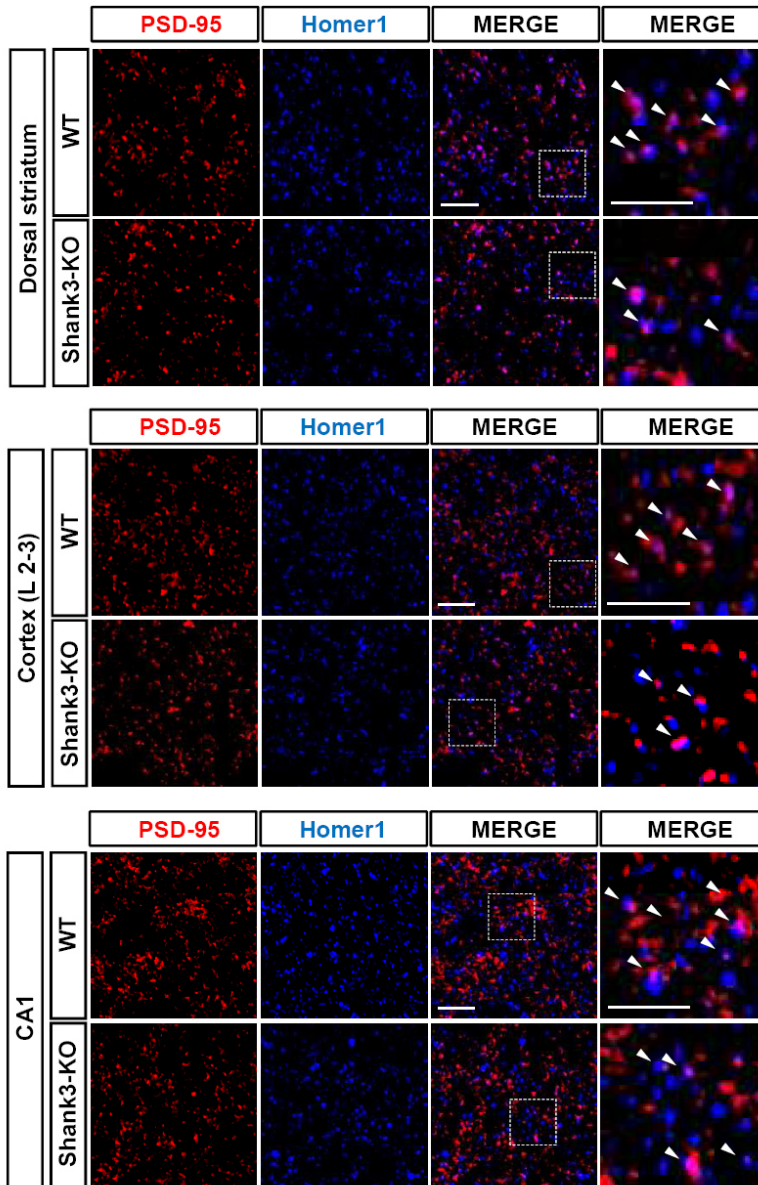
Data are shown as the mean  $\pm$  SEM of 10 animals for each group. \*,  $p < 0.05$ , \*\*;  $p < 0.01$ ; compared to the corresponding WT mice; \$\$,  $p < 0.01$  compared to the corresponding WT mice on the same day; &&,  $p < 0.01$  compared to the same genotype on day 1. Student's t-tests or two-way Anova followed by Bonferroni tests were used for statistical analysis.

Figure 2

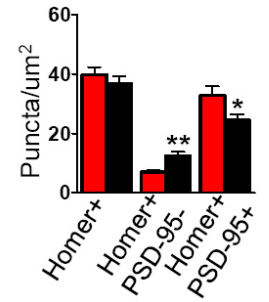
A



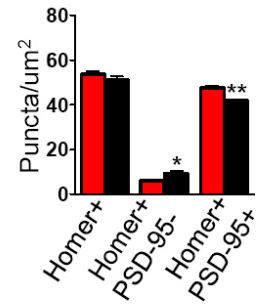
B



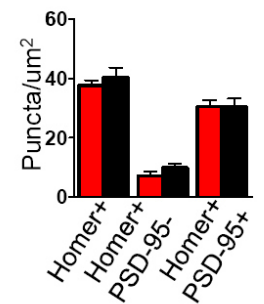
**Dorsal striatum**

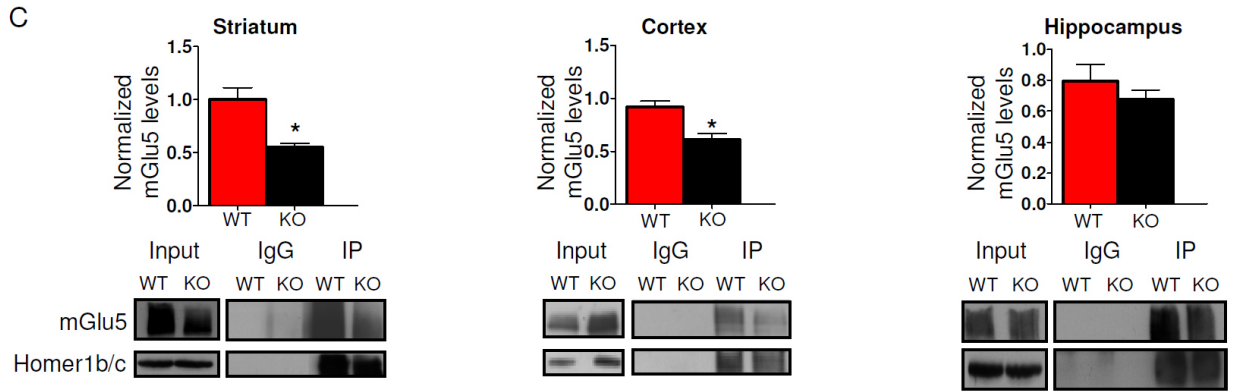


**Cortex (L 2-3)**



**CA1**

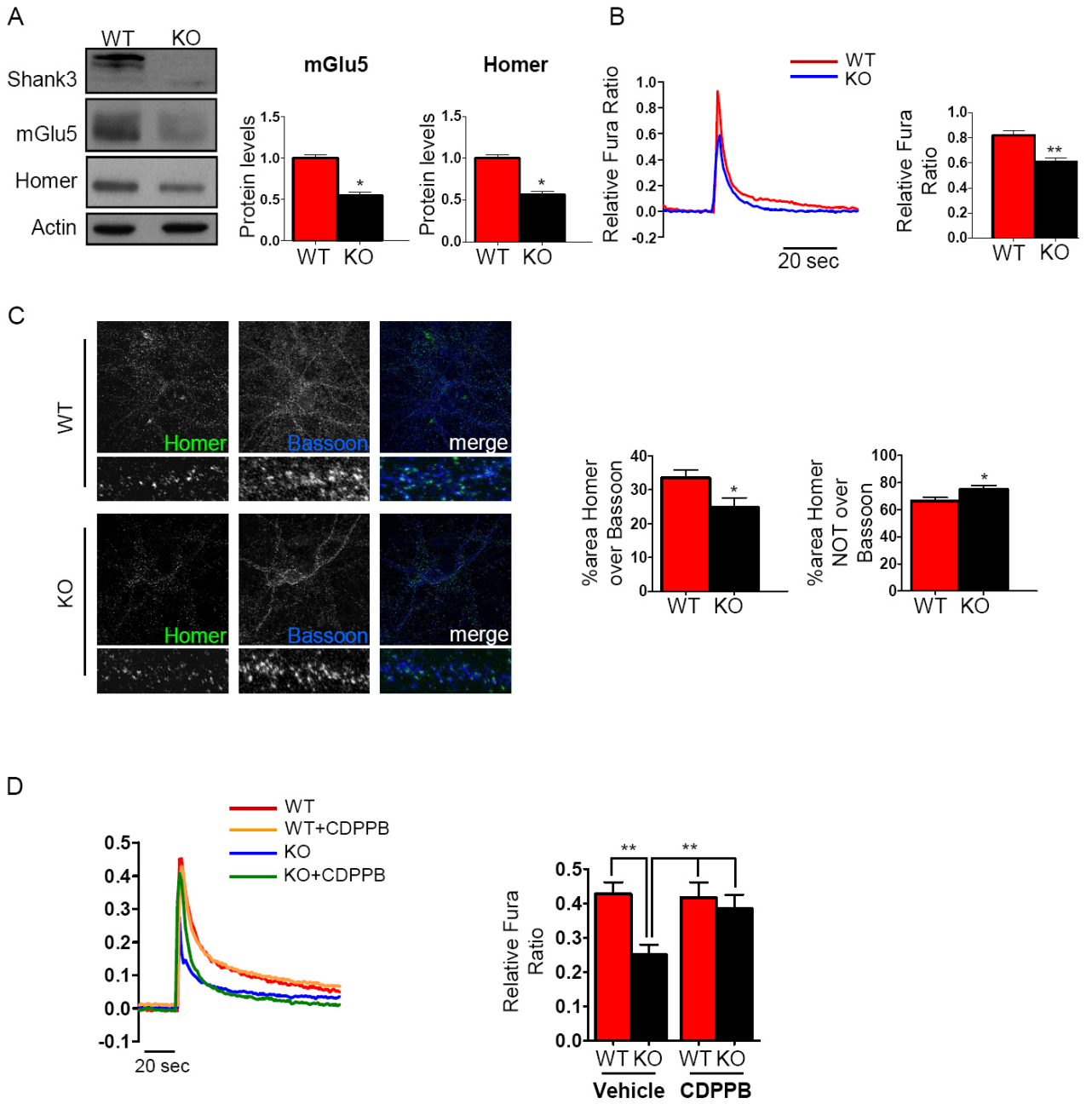




### Figure 2: Shank3 absence alters Homer and mGlu5 synaptic localization

**A)** Protein levels of metabotropic glutamate receptor 5 (mGlu5) and Homer1b/c were analyzed using Western blot analysis in postsynaptic density (PSD) fractions obtained from tissues in the striatum, cortex and hippocampus of wild-type (WT) and *Shank3Δ11<sup>-/-</sup>* mice. Protein levels were each normalized against the respective PSD-95 and ratios were compared between genotypes. The results are shown as bar diagrams, and representative blots are shown below. All data are presented as the mean  $\pm$  SEM; all P-values were derived using unpaired, two-tailed Student's t-tests; \*,  $p < 0.05$ ; \*\*,  $p < 0.01$ . Analyses are based on a sample size of  $n = 6$  animals for each group (WT and KO). **B)** Representative confocal micrographs showing PSD-95 (red) and Homer1 (blue). Co-labeled puncta (arrowheads) are visible in high magnification images. The images show immunofluorescence puncta in the neuropil of the dorsal striatum, layer 2-3 of the primary somatosensory cortex and in the CA1 of the hippocampus in *Shank3Δ11<sup>-/-</sup>* and KO mice. The results are shown as bar diagrams. Data are presented as mean  $\pm$  SEM. \*  $p < 0,05$ ; \*\*  $p < 0,01$ . Scale bars: 5  $\mu\text{m}$  and 3  $\mu\text{m}$ . **C)** PSD-enriched preparations of the striatum, cortex and hippocampus were obtained from three P60 WT and KO mice and subjected to an in vitro coimmunoprecipitation assay using rabbit Homer1b/c antibodies. The immunoprecipitated proteins were revealed after immunoblotting using rabbit mGlu5 and Homer1b/c antibodies. A rabbit IgG antibody was used as the negative control. The data are expressed as the mean  $\pm$  SEM of three independent experiments. \*,  $p < 0.05$ .

Figure 3



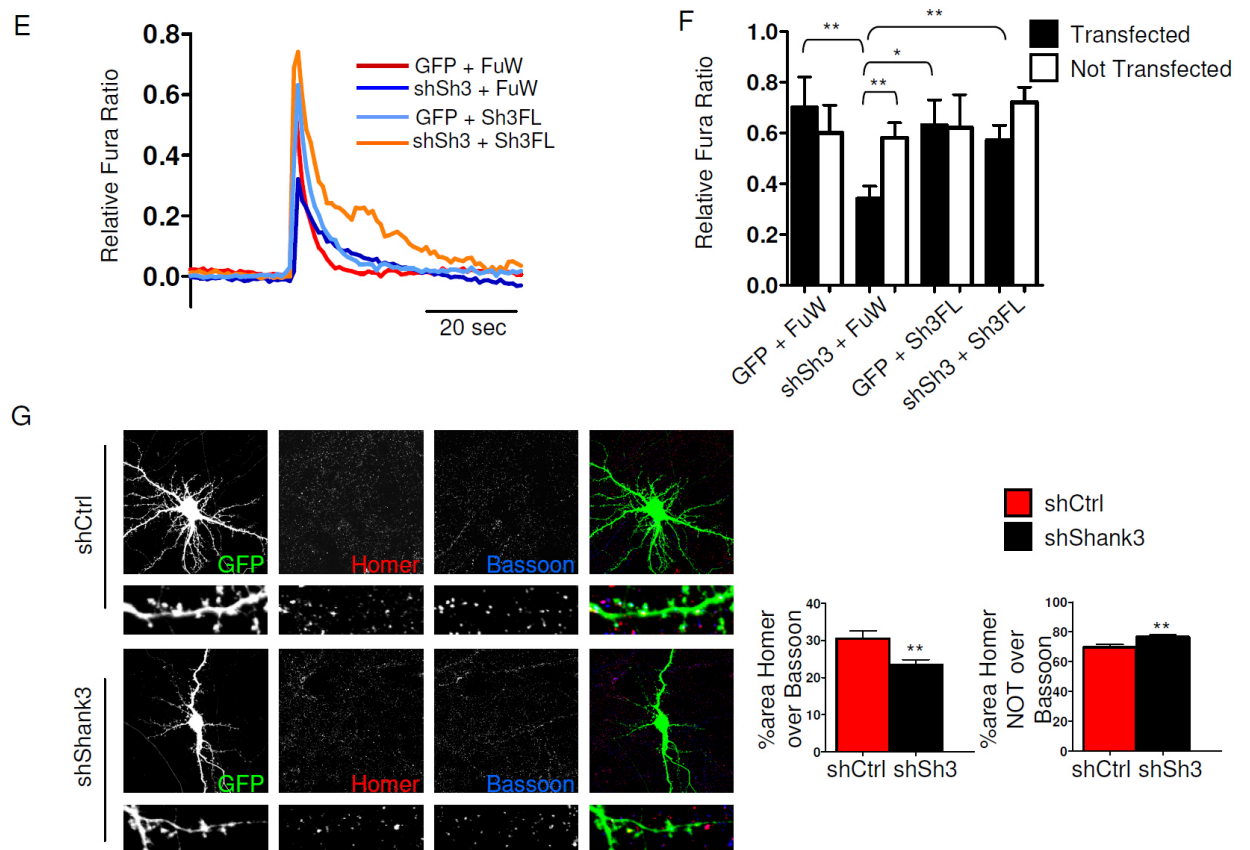


### Figure 3: Shank3 absence impairs mGlu5-mediated intracellular calcium release

Cortical neuronal cultures were prepared from WT and *Shank3* $\Delta 11^{-/-}$  E17-E18 mouse embryos. **A)** Western blot analysis of PSD-enriched fractions of cortical primary neurons obtained from WT and *Shank3* $\Delta 11^{-/-}$  mice at DIV15. Protein levels were each normalized against the respective actin. Data are expressed as the mean  $\pm$  SEM of three independent cultures by genotype. \*,  $p < 0.05$ . **B)** At DIV14-15 neurons were loaded with Fura-2 AM (5  $\mu$ M, 30 min). After 20 min of de-esterification, the neurons were challenged with 200  $\mu$ M DHPG. The results are shown as bar diagrams. Representative traces of  $\text{Ca}^{2+}$  transients are shown on the left, and the data are expressed as the mean  $\pm$  SEM of the indicated numbers of neurons that were registered from 18 coverslips (for each genotype) in three independent cultures. \*,  $p < 0.05$ ; \*\*,  $p < 0.01$ . **C)** Representative images of WT and *Shank3* $\Delta 11^{-/-}$  mouse primary cortical neurons at DIV15. Confocal images were obtained using a Confocal Microscope with a 63x objective and with sequential-acquisition set at a resolution of 1024 x 1024 pixels. A total of 16 WT and *Shank3* $\Delta 11^{-/-}$  primary cortical neurons at DIV15 were randomly chosen for

quantification from 4 to 10 coverslips from three independent experiments. Colocalization measurements were performed using MetaMorph image analysis software. The histogram shows the mean  $\pm$  SEM for the area of Homer clusters (green) over the area of Bassoon clusters (blue) and the area of Homer clusters NOT over Bassoon clusters. \*,  $p < 0.05$ . **D)** At DIV12-14 cortical neurons were loaded with Fura-2 and challenged with 200  $\mu$ M DHPG either in presence (5 min preincubation) or in absence of 3  $\mu$ M CDPPB. Results are shown as bar diagrams. Representative traces of  $Ca^{2+}$  transients are shown left; data are expressed as mean  $\pm$  SEM of indicated numbers of neurons registered from 18 coverslips (for each conditions) in three independent cultures for genotype. \*  $p < 0.05$ ; \*\*  $p < 0.01$ .

**E)** Primary rat cortical neurons were prepared from E18-E19 mouse embryos at DIV11 and transfected with the following combinations of plasmids: GFP and FUW control vector (GFP+FUW); shShank3 plasmid and control FUW vector (shSh3+FUW); GFP and Shank3 full-length mutated to be resistant to shShank3 (GFP+Sh3FL), and shShank3 plasmid plus Shank3 full-length (shSh3+Sh3FL). At DIV14-15, the neurons were loaded with Fura-2 AM (5  $\mu$ M, 30 min) and stimulated with 200  $\mu$ M DHPG. Representative traces of DHPG-induced  $Ca^{2+}$  transients are shown. **F)** Both GFP-expressing (transfected) and non-transduced (non-transf.) neurons were selected for analysis. Data are expressed as the mean  $\pm$  SEM of the indicated numbers of neurons from 6 to 20 coverslips per condition from three independent culture preparations. \*,  $p < 0.05$  and \*\*,  $p < 0.01$ . **G)** Representative images of rat cortical neurons that were transfected with shCtrl (control vector) and shShank3 constructs. In all, 6 primary rat neurons that were transfected at DIV11 and fixed at DIV 15 for each construct were randomly chosen for quantification from 4 to 10 coverslips from three independent experiments. Colocalization measurements were performed using MetaMorph image analysis software. The histogram shows the mean  $\pm$  SEM of the area of Homer clusters (red) over the area of Bassoon clusters (blue) and the area of Homer clusters NOT over area of Bassoon clusters. \*\*,  $p < 0.01$

Figure 4

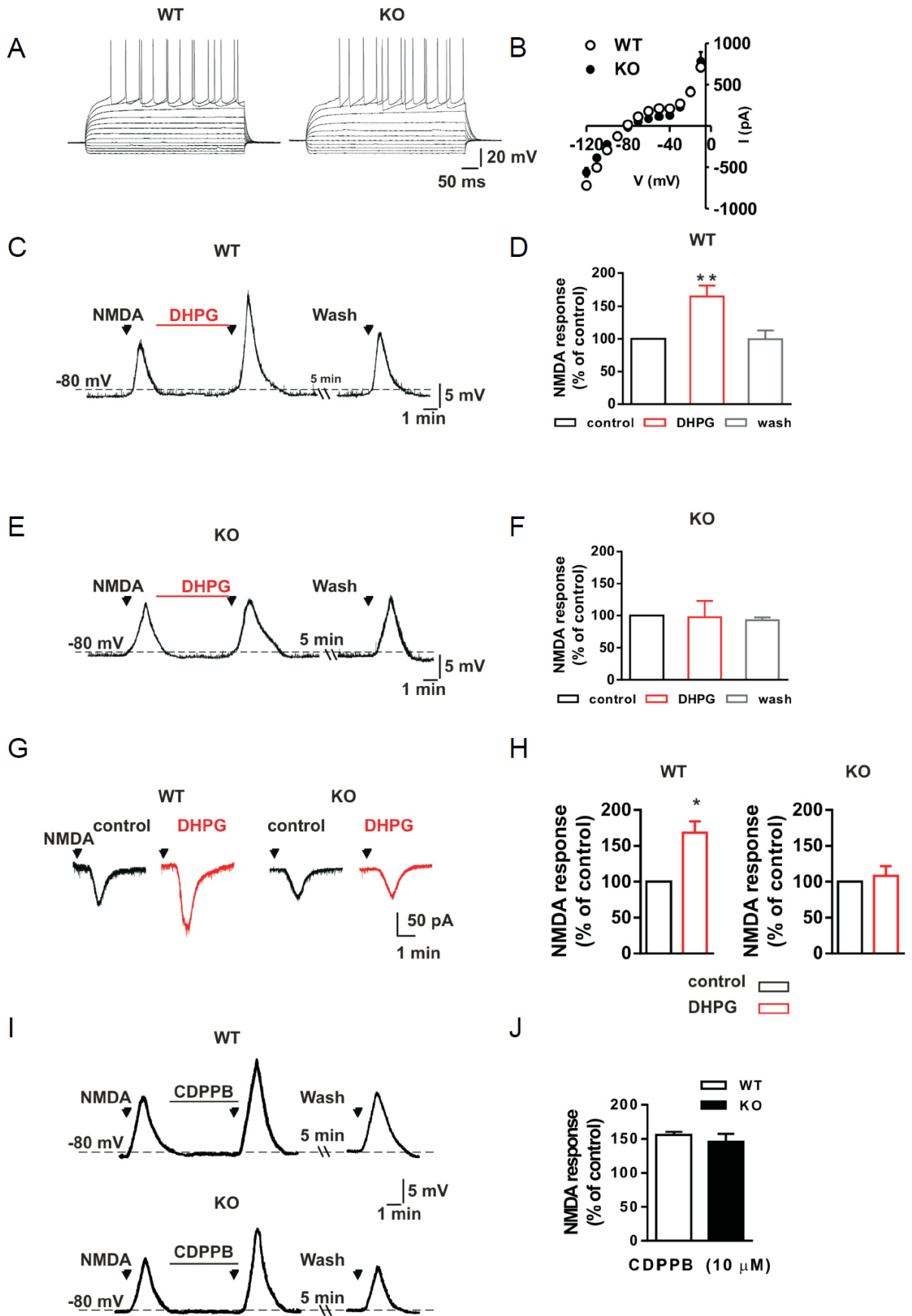


#### **Figure 4: The effect of mGlu5 stimulation on NMDA responses in striatal medium spiny neurons is dependent on Shank3**

Because we observed a disruption in synaptic Homer localization in the absence of Shank3 and high expression of Shank3 in the striatum, we tested the electrophysiological properties of striatal neurons.

Patch-clamp recordings were obtained using medium spiny neurons (MSNs) obtained from WT and KO mice to explore whether the deletion of Shank3 affected the basal membrane properties of striatal neurons. Current-voltage curves were obtained by delivering hyperpolarizing and depolarizing steps of currents to the MSNs of KO (n=6) and WT (n=6) mice, and we observed no difference between these two groups of neurons, suggesting that the basal membrane properties of MSNs do not depend on Shank3 expression (**Figure 4 A-B**).

We subsequently studied whether Shank3 was responsible for the observed changes in the membrane potential and the ionic currents induced by the stimulation of group I mGlu receptors in MSNs. Activation of these types of metabotropic glutamate receptors has been shown to enhance the membrane depolarization/inward current that is produced by the activation of the NMDA receptor in striatal MSNs. As shown in **Figures 4C and 4G**, the application of 30  $\mu$ M NMDA produced a membrane depolarization of approximately 15 mV and an inward current of approximately -70 pA in MSNs in WT mice, while the co-application of NMDA in the presence of DHPG produced a significantly larger depolarization (**Figure 4C-D**) and inward current (**Figure 4 G-H**). Interestingly, in the MSNs obtained from KO mice, the co-application of NMDA plus DHPG failed to produce a membrane depolarization and inward current that was larger than those observed in the presence of NMDA alone (**Fig. 4E-H**).

We then tested the effect of CDPPB on MSNs obtained from WT and KO mice, and as shown in **Figures 4I-J**, CDPPB treatment was able to recover normal NMDA receptor functions, which depend on mGlu5 receptor activity, in the MSNs obtained from Shank3 KO mice to levels comparable to those in the MSNs obtained from WT mice.

Figure 5

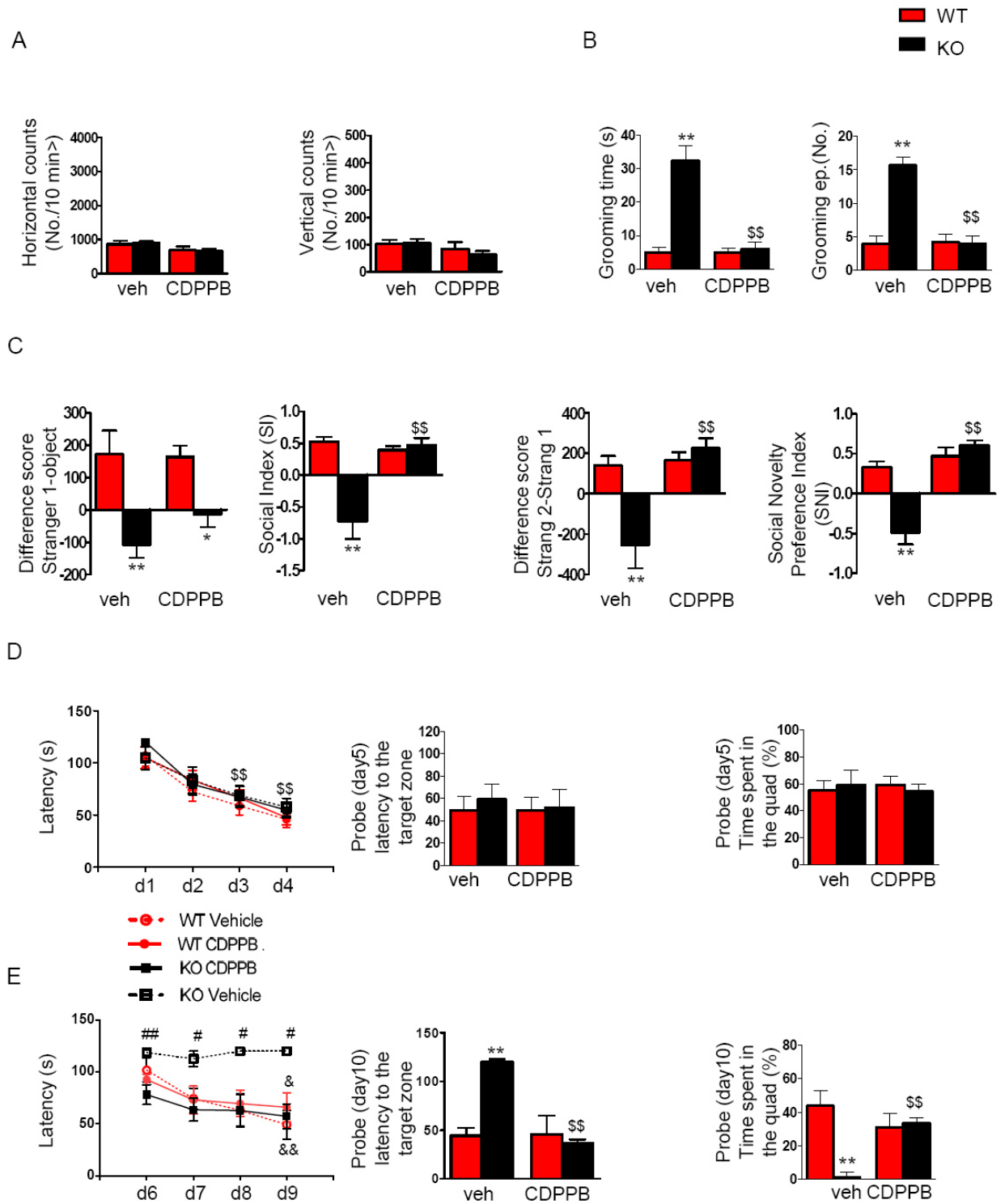


**Figure 5: CDPPB is able to rescue ASD-like behaviors in *Shank3Δ11*<sup>-/-</sup> mice**

The behavioral phenotypes of *Shank3Δ11*<sup>-/-</sup> mice were evaluated after CDPPB (3 mg/kg i.p.) or vehicle (veh) treatments. Both compounds were administered acutely or

chronically at 70 min before each test. **A)** Mean horizontal (left) and vertical (right) movements were recorded for 10 min in an automated activity cage immediately after grooming recording. **B)** Self-grooming behaviors were evaluated as the time spent grooming (left) and the total number of grooming episodes (right) after acute treatment with CDPPB or vehicle. **C)** Differences in the scores corresponding to the time spent in the chamber associated with the never-seen-before mouse and the empty cage (left) or the familiar mouse (preference for social novelty test) (right). **D-E)** Acquisition and reversal tasks in the Morris water maze were performed after daily treatments for the duration of the task during both acquisition and reversal in mice administered CDPPB or vehicle to analyze learning patterns (left), escape latency to the target zone (center) and the time spent in the quadrant (right) during the probe test.

The data are shown as the mean  $\pm$  SEM of 10 animals for each group. \*,  $p < 0.05$ ; \*\*,  $p < 0.01$  compared to the corresponding WT mice; \$\$,  $p < 0.01$  compared to the corresponding Shank3 exon 11 KO mice that were treated with vehicle; #,  $p < 0.05$  and ##,  $p < 0.01$  compared to the Shank3 exon 11 KO mice that were treated with CDPPB. &,  $p < 0.05$  and &&,  $p < 0.01$  compared to the same genotype on day 1 (two-way Anova followed by Bonferroni test).

Figure 6

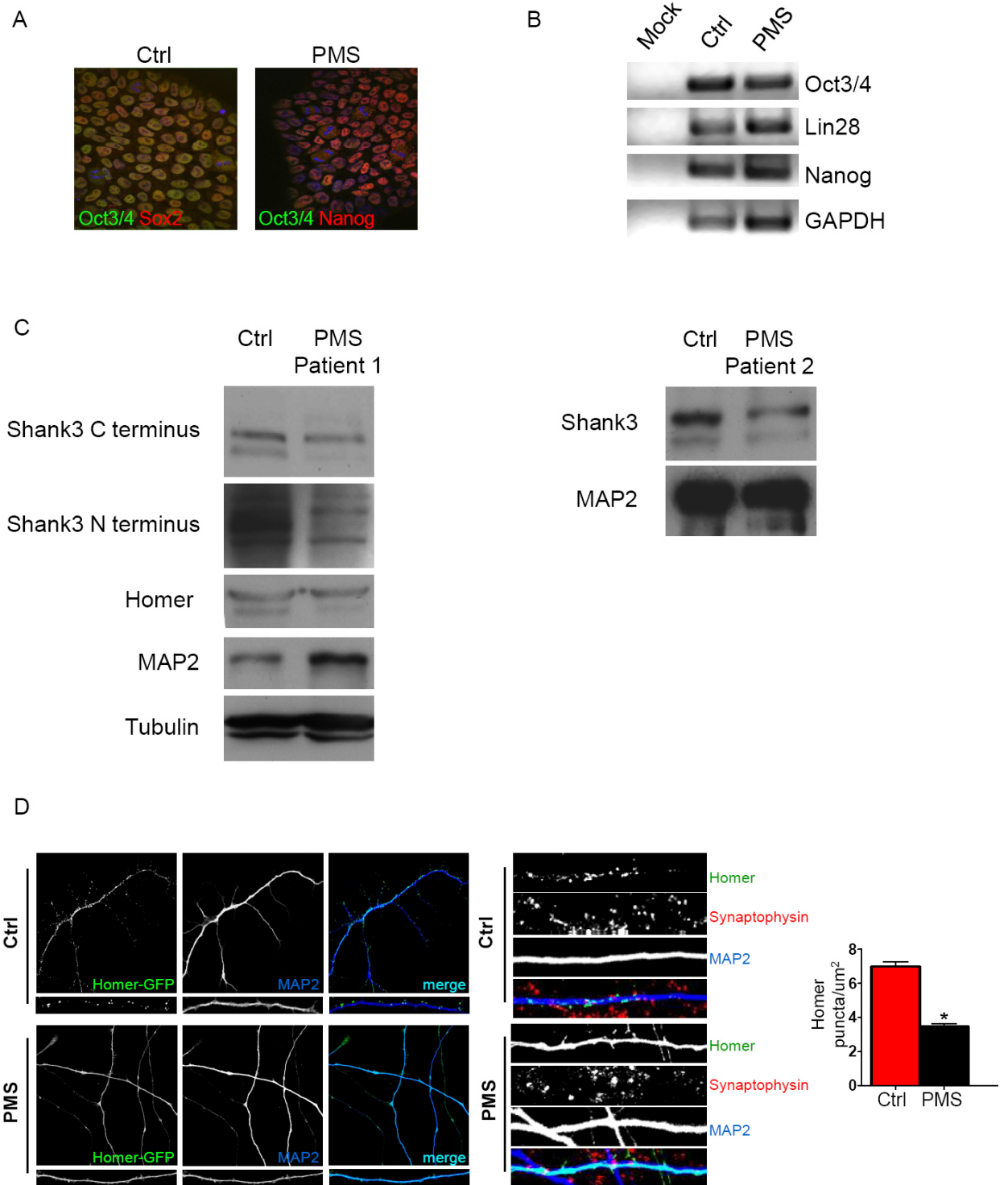


**Figure 6: Shank3 absence causes alterations of Homer localization in neurons derived from patients affected by Phelan McDermid Syndrome (PMS)**

**A)** Representative images of Ctrl and PMS derived hiPSC colonies, clones. **A-B)** All selected clones are positive for pluripotency markers as shown by immunofluorescence panel **A** and PCR panel **B**. **C)** Western blot of Shank3 protein expression in neurons obtained from NPC of control and PMS patients differentiated for 80 days. Patient 1, left; Patient 2 right. **D)** The panels show representative images of hNP-derived neurons and dendrites, which, after infection with a lentivirus expressing Homer-GFP, were differentiated in neuronal differentiation medium for 80 days. The staining (right panel) shows that GFP-Homer1b clusters in iPSC-derived neurons colocalize with the presynaptic marker synaptophysin. The results are shown as bar diagrams. The data are presented as the mean  $\pm$  SEM. \*,  $p < 0.05$ .

## ***DISCUSSION***

Phelan-McDermid (PMS or 22q13.3 deletion syndrome) syndrome is a rare genetic disorder that causes a severe form of intellectual disability (ID), expressive language delays and other autistic features.

PMS results from the loss of the distal long arm of chromosome 22, in particular the 22q13.3 region.

The chromosome 22 breakpoint is located precisely within the exon 21 of the human homologue of the ProSAP2 gene, *SHANK3*, and it has been demonstrated that the majority of 22q13.3 deletion syndrome neurological deficits are related to haploinsufficiency of *SHANK3* gene.

Furthermore *SHANK3* truncating mutations have been reported in patients with autism spectrum disorders (ASD) (Moessner et al., 2007, Nemirovsky et al., 2015, Hara et al., 2015, Cochoy et al., 2015). ASDs are a group of neurodevelopmental disorders including autism, Asperger syndrome, childhood disintegrative disorder, and pervasive developmental disorder not otherwise specified (Liu and Scott, 2014). ASD is defined by two main behavioral features: repetitive/restricted behavioral patterns and impaired sociability and communication.

Considering the relevant role of Shank3 in these disorders, the study of Shank3 function in the brain is crucial to identify new pharmacological targets for treating patients affected by *SHANK3* mutations or deletions.

For this reason in the last years seven Shank3 KO mouse models have been generated, deleting different regions of the gene (Peça et al., 2011, Schmeisser et al., 2012, Bozdagi et al., 2010, Wang et al., 2011, Kouser et al., 2013, Lee et al., 2015).

Shank3 is one of the most important scaffolding proteins at postsynaptic density of excitatory synapses. Thanks to its multiple domains is able to connect each other a large number of proteins including other scaffolding proteins, actin-binding proteins and glutamate receptors.

For this reason Shank3 plays an important role in the proper establishment and maintenance of synaptic contacts and plasticity.

To study the role of Shank3 in synapse function and to develop therapies that might ameliorate the neuropsychiatric symptoms found in patients with PMS or other mutations in the *SHANK3* gene, we characterized the behavioral, molecular and electrophysiological phenotypes of *Shank3* mutant mice that were generated by

deleting the exon 11 (Schmeisser et al., 2012). Among the *Shank3* mutants that were available, *Shank3Δ11<sup>-/-</sup>* mice are less often studied, although they are highly homologous to the *Shank3B<sup>-/-</sup>* mutants, lacking the PDZ domain described by Peça et al. (Peça et al., 2011).

From the behavioral analyses we found that *Shank3Δ11<sup>-/-</sup>* mice present an increased self grooming behavior and impaired social interaction, so the two main features of ASD, suggesting that this is a good model to study the role of Shank3 in the pathogenesis of PMS and ASD.

Shank proteins interact with group I of metabotropic receptors, which includes mGlu5, through the binding to Homer1 scaffold proteins.

We focused our attention on the analysis of mGlu5 and Homer protein levels, because our previous data showed a reduce expression of mGlu5 in Shank3 knock-down neurons (Verpelli et al., 2011). In *Shank3Δ11<sup>-/-</sup>* mice we found a reduction of the protein expression levels of mGlu5 and Homer1b/c in cortex and striatum.

Our biochemical and morphological data demonstrate that in *Shank3Δ11<sup>-/-</sup>* mice, the localization of Homer1b/c to the PSD is significantly reduced in two different brain areas: striatum and cortex. This lead to a consequent reduction of the synaptic association between Homer1b/c and mGlu5 in these specific brain regions.

The reduction of Homer expression is a common alteration found in different Shank3 mutants (Wang et al., 2011, Peça et al., 2011).

In addition our data indicate that Shank3 in different brain regions could have different functions at synapses.

This brain-region specificity of Shank3 in regulating glutamate receptor levels at synapses, have been observed also in other Shank3 mutant mice (Wang et al., 2011, Peça et al., 2011), suggesting that splice variants have a crucial role in this process.

Shank3 is important for Homer1b/c clustering at synapses also in human neurons, indeed we demonstrated that Homer1b/c cluster formation is impaired in hiPSC-derived neurons obtained from patients affected by PMS, suggesting that Shank3 is also important for the normal clustering of Homer1b/c into synaptic puncta in human neurons.

Homer physically and functionally links mGlu5 receptors to their downstream effectors, the IP3 receptors, allowing a more efficient release of intracellular calcium in response to receptor stimulation, so Homer-mGlu5 complex formation is necessary for the correct functionality of mGlu receptors (Ronesi et al., 2012).

We demonstrated *in vitro* that mGlu5-dependent  $Ca^{2+}$  release from intracellular stores is impaired in cortical neurons obtained from *Shank3 $\Delta$ 11<sup>-/-</sup>* mice and we further provided *in vivo* data in which mGlu5-dependent NMDA receptor potentiation is completely abolished in striatal medium spiny neurons of *Shank3 $\Delta$ 11<sup>-/-</sup>* mice.

The importance of Shank3 in regulating mGlu5 signaling is also supported by the fact that the expression of shRNA-resistant Shank3 rescued the changes in DHPG-induced  $Ca^{2+}$  release from intracellular stores observed in Shank3 knocked down cortical neurons.

We also provided the evidences that CDPBB induced the positive modulation of mGlu5 activity and rescued the functional deficits observed in both cortical and striatal neurons in *Shank3 $\Delta$ 11<sup>-/-</sup>* mice.

Taken together these data demonstrate that the absence of Shank3 causes principally an alteration of group I mGlu receptors mediated synaptic signaling in specific brain areas.

Recent studies reported that the inhibition of mGlu-Homer complex formation impairs mGlu receptors-dependent LTD and protein synthesis in normal mice (Ronesi et al., 2012).

In a mouse model of Fragile- X syndrome, mGlu5 receptors are less associated with Homer1b/c and more associated with Homer1a (Giuffrida et al., 2005, Ronesi et al., 2012), that interferes with the cross-linking activity of Homer1b/c (Hayashi et al., 2009).

Similarly, in a mouse model of Angelman Syndrome, mGlu5 receptor-dependent synaptic plasticity was altered because it showed an increased association with Homer 1b/c (Pignatelli et al., 2014).

In these two models an enhancement of hippocampal mGlu5 receptor function is the main phenotype, while in our mouse model is exactly the opposite, indeed we observed a decrease of mGlu5 receptor function.

This indicates that if mGlu5 signaling is pathologically modified in any direction (enhancement or reduction) this causes an alteration of synapse function.

Recently it has been also identified *HOMER1* as a novel risk gene for non-syndromic ASD (Kelleher et al., 2012) and it has been showed that mGlu5 gene expression is reduced within the dorsolateral prefrontal cortex of ASD patients (Chana et al., 2015).

Because all our findings underlined and confirmed a critical impairment on Shank3-Homer-mGlu5 complex, we decided to test if ASD-like behaviors of *Shank3 $\Delta$ 11<sup>-/-</sup>* mice can be reversed by the treatment with CDPPB, an allosteric positive modulator of mGlu5.

The, *in vivo*, treatment with CDPPB is able to rescue repetitive behavior, cognitive rigidity and partially social interaction.

Importantly the potential of mGlu5 PAM has already been tested in other models of ASD. Indeed CDPPB restored synaptic and behavioral deficits in mouse models of tuberousclerosis syndrome (TSC), a genetic syndrome associated to ASD and ID (Auerbach et al., 2011), and very recently CDPPB administration ameliorated the behavioral deficits reported in Sarm1 knockdown mice (Lin et al., 2014). In addition in a mouse model lacking exon 4-6 of *SHANK2* gene, that presents ASD-like phenotypes, the treatment with CDPPB normalized some behavioral deficits (Won et al., 2012).

Our data show that the use of a positive allosteric modulators of mGlu5, such as CDPPB, antagonizes ASD-like behaviors and suggests that mGlu5 activity could be envisaged as a potential therapeutic target for neurodevelopmental disorders in general, as suggested by many recent studies (Nickols and Conn, 2014).

Concluding in our work we demonstrated that the deletion of exon 11 of *SHANK3* gene in mice leads to ASD like behaviors and that in this mouse model Shank3 plays a major role in modulating mGlu5 signaling by regulating Homer recruitment/localization to the PSD specifically in cortex and striatum, two brain regions that are highly associated to ASD-like behaviors.

## ***REFERENCES***

- Attucci S, Carlà V, Mannaioni G, Moroni F (2001) Activation of type 5 metabotropic glutamate receptors enhances NMDA responses in mice cortical wedges. *Br J Pharmacol* 132:799-806.
- Auerbach BD, Osterweil EK, Bear MF (2011) Mutations causing syndromic autism define an axis of synaptic pathophysiology. *Nature* 480:63-68.
- Bates B, Xie Y, Taylor N, Johnson J, Wu L, Kwak S, Blatcher M, Gulukota K, Paulsen JE (2002) Characterization of mGluR5R, a novel, metabotropic glutamate receptor 5-related gene. *Brain Res Mol Brain Res* 109:18-33.
- Bear MF, Huber KM, Warren ST (2004) The mGluR theory of fragile X mental retardation. *Trends Neurosci* 27:370-377.
- Bevins RA, Besheer J (2006) Object recognition in rats and mice: a one-trial non-matching-to-sample learning task to study 'recognition memory'. *Nat Protoc* 1:1306-1311.
- Bigge CF (1999) Ionotropic glutamate receptors. *Curr Opin Chem Biol* 3:441-447.
- Boccuto L, Lauri M, Sarasua SM, Skinner CD, Buccella D, Dwivedi A, Orteschi D, Collins JS, Zollino M, Visconti P, Dupont B, Tiziano D, Schroer RJ, Neri G, Stevenson RE, Gurrieri F, Schwartz CE (2013) Prevalence of SHANK3 variants in patients with different subtypes of autism spectrum disorders. *Eur J Hum Genet* 21:310-316.
- Boeckers TM, Bockmann J, Kreutz MR, Gundelfinger ED (2002) ProSAP/Shank proteins - a family of higher order organizing molecules of the postsynaptic density with an emerging role in human neurological disease. *J Neurochem* 81:903-910.
- Boeckers TM, Kreutz MR, Winter C, Zuschratter W, Smalla KH, Sanmarti-Vila L, Wex H, Langnaese K, Bockmann J, Garner CC, Gundelfinger ED (1999) Proline-rich synapse-associated protein-1/cortactin binding protein 1 (ProSAP1/CortBP1) is a PDZ-domain protein highly enriched in the postsynaptic density. *J Neurosci* 19:6506-6518.
- Bonaglia MC, Giorda R, Borgatti R, Felisari G, Gagliardi C, Selicorni A, Zuffardi O (2001) Disruption of the ProSAP2 gene in a t(12;22)(q24.1;q13.3) is associated with the 22q13.3 deletion syndrome. *Am J Hum Genet* 69:261-268.
- Bonsi P, Cuomo D, De Persis C, Centonze D, Bernardi G, Calabresi P, Pisani A (2005) Modulatory action of metabotropic glutamate receptor (mGluR) 5 on mGluR1

- function in striatal cholinergic interneurons. *Neuropharmacology* 49 Suppl 1:104-113.
- Bozdagi O, Sakurai T, Papapetrou D, Wang X, Dickstein DL, Takahashi N, Kajiwara Y, Yang M, Katz AM, Scattoni ML, Harris MJ, Saxena R, Silverman JL, Crawley JN, Zhou Q, Hof PR, Buxbaum JD (2010) Haploinsufficiency of the autism-associated Shank3 gene leads to deficits in synaptic function, social interaction, and social communication. *Mol Autism* 1:15.
- Bozdagi O, Tavassoli T, Buxbaum JD (2013) Insulin-like growth factor-1 rescues synaptic and motor deficits in a mouse model of autism and developmental delay. *Mol Autism* 4:9.
- Calabresi P, Pisani A, Mercuri NB, Bernardi G (1992) Long-term Potentiation in the Striatum is Unmasked by Removing the Voltage-dependent Magnesium Block of NMDA Receptor Channels. *Eur J Neurosci* 4:929-935.
- Canitano R (2014) New experimental treatments for core social domain in autism spectrum disorders. *Front Pediatr* 2:61.
- Carbonetto S (2014) A blueprint for research on Shankopathies: a view from research on autism spectrum disorder. *Dev Neurobiol* 74:85-112.
- Cartmell J, Schoepp DD (2000) Regulation of neurotransmitter release by metabotropic glutamate receptors. *J Neurochem* 75:889-907.
- Chana G, Laskaris L, Pantelis C, Gillett P, Testa R, Zantomio D, Burrows EL, Hannan AJ, Everall IP, Skafidas E (2015) Decreased expression of mGluR5 within the dorsolateral prefrontal cortex in autism and increased microglial number in mGluR5 knockout mice: Pathophysiological and neurobehavioral implications. *Brain Behav Immun* 49:197-205.
- Chen Y, Nong Y, Goudet C, Hemstapat K, de Paulis T, Pin JP, Conn PJ (2007) Interaction of novel positive allosteric modulators of metabotropic glutamate receptor 5 with the negative allosteric antagonist site is required for potentiation of receptor responses. *Mol Pharmacol* 71:1389-1398.
- Cheng J, Dong J, Cui Y, Wang L, Wu B, Zhang C (2012) Interacting partners of AMPA-type glutamate receptors. *J Mol Neurosci* 48:441-447.
- Chu Z, Hablitz JJ (2000) Quisqualate induces an inward current via mGluR activation in neocortical pyramidal neurons. *Brain Res* 879:88-92.

- Cleva RM, Olive MF (2011) Positive allosteric modulators of type 5 metabotropic glutamate receptors (mGluR5) and their therapeutic potential for the treatment of CNS disorders. *Molecules* 16:2097-2106.
- Cochoy DM, Kolevzon A, Kajiwara Y, Schoen M, Pascual-Lucas M, Lurie S, Buxbaum JD, Boeckers TM, Schmeisser MJ (2015) Phenotypic and functional analysis of SHANK3 stop mutations identified in individuals with ASD and/or ID. *Mol Autism* 6:23.
- Conn PJ, Lindsley CW, Jones CK (2009) Activation of metabotropic glutamate receptors as a novel approach for the treatment of schizophrenia. *Trends Pharmacol Sci* 30:25-31.
- Conn PJ, Tamminga C, Schoepp DD, Lindsley C (2008) Schizophrenia: moving beyond monoamine antagonists. *Mol Interv* 8:99-107.
- Costales JL, Kolevzon A (2015) Phelan-McDermid Syndrome and SHANK3: Implications for Treatment. *Neurotherapeutics* 12:620-630.
- D'Antoni S, Spatuzza M, Bonaccorso CM, Musumeci SA, Ciranna L, Nicoletti F, Huber KM, Catania MV (2014) Dysregulation of group-I metabotropic glutamate (mGlu) receptor mediated signalling in disorders associated with Intellectual Disability and Autism. *Neurosci Biobehav Rev* 46 Pt 2:228-241.
- Dhar SU, del Gaudio D, German JR, Peters SU, Ou Z, Bader PI, Berg JS, Blazo M, Brown CW, Graham BH, Grebe TA, Lalani S, Irons M, Sparagana S, Williams M, Phillips JA, Beaudet AL, Stankiewicz P, Patel A, Cheung SW, Sahoo T (2010) 22q13.3 deletion syndrome: clinical and molecular analysis using array CGH. *Am J Med Genet A* 152A:573-581.
- Distler U, Schmeisser MJ, Pelosi A, Reim D, Kuharev J, Weiczner R, Baumgart J, Boeckers TM, Nitsch R, Vogt J, Tenzer S (2014) In-depth protein profiling of the postsynaptic density from mouse hippocampus using data-independent acquisition proteomics. *Proteomics* 14:2607-2613.
- Durand CM, Betancur C, Boeckers TM, Bockmann J, Chaste P, Fauchereau F, Nygren G, Rastam M, Gillberg IC, Anckarsäter H, Sponheim E, Goubran-Botros H, Delorme R, Chabane N, Mouren-Simeoni MC, de Mas P, Bieth E, Rogé B, Héron D, Burglen L, Gillberg C, Leboyer M, Bourgeron T (2007) Mutations in the gene encoding the synaptic scaffolding protein SHANK3 are associated with autism spectrum disorders. *Nat Genet* 39:25-27.

- Ebrahimi S, Okabe S (2014) Structural dynamics of dendritic spines: molecular composition, geometry and functional regulation. *Biochim Biophys Acta* 1838:2391-2398.
- Ethell IM, Pasquale EB (2005) Molecular mechanisms of dendritic spine development and remodeling. *Prog Neurobiol* 75:161-205.
- Foa L, Gasperini R (2009) Developmental roles for Homer: more than just a pretty scaffold. *J Neurochem* 108:1-10.
- Freudenthal R, Romano A, Routtenberg A (2004) Transcription factor NF-kappaB activation after in vivo perforant path LTP in mouse hippocampus. *Hippocampus* 14:677-683.
- Giuffrida R, Musumeci S, D'Antoni S, Bonaccorso CM, Giuffrida-Stella AM, Oostra BA, Catania MV (2005) A reduced number of metabotropic glutamate subtype 5 receptors are associated with constitutive homer proteins in a mouse model of fragile X syndrome. *J Neurosci* 25:8908-8916.
- Giustetto M, Kirsch J, Fritschy JM, Cantino D, Sassoè-Pognetto M (1998) Localization of the clustering protein gephyrin at GABAergic synapses in the main olfactory bulb of the rat. *J Comp Neurol* 395:231-244.
- Grabrucker AM, Knight MJ, Proepper C, Bockmann J, Joubert M, Rowan M, Nienhaus GU, Garner CC, Bowie JU, Kreutz MR, Gundelfinger ED, Boeckers TM (2011a) Concerted action of zinc and ProSAP/Shank in synaptogenesis and synapse maturation. *EMBO J* 30:569-581.
- Grabrucker AM, Schmeisser MJ, Schoen M, Boeckers TM (2011b) Postsynaptic ProSAP/Shank scaffolds in the cross-hair of synaptopathies. *Trends Cell Biol* 21:594-603.
- Guilmatre A, Huguet G, Delorme R, Bourgeron T (2014) The emerging role of SHANK genes in neuropsychiatric disorders. *Dev Neurobiol* 74:113-122.
- Gundelfinger ED, Boeckers TM, Baron MK, Bowie JU (2006) A role for zinc in postsynaptic density assembly and plasticity? *Trends Biochem Sci* 31:366-373.
- Halberstadt AL, Lehmann-Masten VD, Geyer MA, Powell SB (2011) Interactive effects of mGlu5 and 5-HT2A receptors on locomotor activity in mice. *Psychopharmacology (Berl)* 215:81-92.
- Han K, Holder JL, Schaaf CP, Lu H, Chen H, Kang H, Tang J, Wu Z, Hao S, Cheung SW, Yu P, Sun H, Breman AM, Patel A, Lu HC, Zoghbi HY (2013) SHANK3

- overexpression causes manic-like behaviour with unique pharmacogenetic properties. *Nature* 503:72-77.
- Hara M, Ohba C, Yamashita Y, Saitsu H, Matsumoto N, Matsuishi T (2015) De novo SHANK3 mutation causes Rett syndrome-like phenotype in a female patient. *Am J Med Genet A* 167:1593-1596.
- Harris KM, Weinberg RJ (2012) Ultrastructure of synapses in the mammalian brain. *Cold Spring Harb Perspect Biol* 4.
- Hayashi MK, Ames HM, Hayashi Y (2006) Tetrameric hub structure of postsynaptic scaffolding protein homer. *J Neurosci* 26:8492-8501.
- Hayashi MK, Tang C, Verpelli C, Narayanan R, Stearns MH, Xu RM, Li H, Sala C, Hayashi Y (2009) The postsynaptic density proteins Homer and Shank form a polymeric network structure. *Cell* 137:159-171.
- Hubert GW, Paquet M, Smith Y (2001) Differential subcellular localization of mGluR1a and mGluR5 in the rat and monkey Substantia nigra. *J Neurosci* 21:1838-1847.
- Jiang YH, Ehlers MD (2013) Modeling autism by SHANK gene mutations in mice. *Neuron* 78:8-27.
- Kandel ER, Schwartz JH, Jessell TM, (2013) Principles of Neural Science New York, McGraw-Hill Medical
- Kelleher RJ, Geigenmüller U, Hovhannisyan H, Trautman E, Pinard R, Rathmell B, Carpenter R, Margulies D (2012) High-throughput sequencing of mGluR signaling pathway genes reveals enrichment of rare variants in autism. *PLoS One* 7:e35003.
- Kenney JW, Adoff MD, Wilkinson DS, Gould TJ (2011) The effects of acute, chronic, and withdrawal from chronic nicotine on novel and spatial object recognition in male C57BL/6J mice. *Psychopharmacology (Berl)* 217:353-365.
- Kew JN, Kemp JA (2005) Ionotropic and metabotropic glutamate receptor structure and pharmacology. *Psychopharmacology (Berl)* 179:4-29.
- Kouser M, Speed HE, Dewey CM, Reimers JM, Widman AJ, Gupta N, Liu S, Jaramillo TC, Bangash M, Xiao B, Worley PF, Powell CM (2013) Loss of predominant Shank3 isoforms results in hippocampus-dependent impairments in behavior and synaptic transmission. *J Neurosci* 33:18448-18468.
- Leblond CS, Nava C, Polge A, Gauthier J, Huguet G, Lumbroso S, Giuliano F, Stordeur C, Depienne C, Mouzat K, Pinto D, Howe J, Lemièrre N, Durand CM, Guibert J, Ey E, Toro R, Peyre H, Mathieu A, Amsellem F, Rastam M, Gillberg IC, Rappold

- GA, Holt R, Monaco AP, Maestrini E, Galan P, Heron D, Jacquette A, Afenjar A, Rastetter A, Brice A, Devillard F, Assouline B, Laffargue F, Lespinasse J, Chiesa J, Rivier F, Bonneau D, Regnault B, Zelenika D, Delepine M, Lathrop M, Sanlaville D, Schluth-Bolard C, Edery P, Perrin L, Tabet AC, Schmeisser MJ, Boeckers TM, Coleman M, Sato D, Szatmari P, Scherer SW, Rouleau GA, Betancur C, Leboyer M, Gillberg C, Delorme R, Bourgeron T (2014) Meta-analysis of SHANK Mutations in Autism Spectrum Disorders: a gradient of severity in cognitive impairments. *PLoS Genet* 10:e1004580.
- Lee J, Chung C, Ha S, Lee D, Kim DY, Kim H, Kim E (2015) Shank3-mutant mice lacking exon 9 show altered excitation/inhibition balance, enhanced rearing, and spatial memory deficit. *Front Cell Neurosci* 9:94.
- Lin CW, Chen CY, Cheng SJ, Hu HT, Hsueh YP (2014) Sarm1 deficiency impairs synaptic function and leads to behavioral deficits, which can be ameliorated by an mGluR allosteric modulator. *Front Cell Neurosci* 8:87.
- Liu EY, Scott CT (2014) Great expectations: autism spectrum disorder and induced pluripotent stem cell technologies. *Stem Cell Rev* 10:145-150.
- MacDermott AB, Mayer ML, Westbrook GL, Smith SJ, Barker JL (1986) NMDA-receptor activation increases cytoplasmic calcium concentration in cultured spinal cord neurones. *Nature* 321:519-522.
- Marino MJ, Conn PJ (2002) Direct and indirect modulation of the N-methyl D-aspartate receptor. *Curr Drug Targets CNS Neurol Disord* 1:1-16.
- Martin LJ, Blackstone CD, Haganir RL, Price DL (1992) Cellular localization of a metabotropic glutamate receptor in rat brain. *Neuron* 9:259-270.
- McFarlane HG, Kusek GK, Yang M, Phoenix JL, Bolivar VJ, Crawley JN (2008) Autism-like behavioral phenotypes in BTBR T+tf/J mice. *Genes Brain Behav* 7:152-163.
- Moessner R, Marshall CR, Sutcliffe JS, Skaug J, Pinto D, Vincent J, Zwaigenbaum L, Fernandez B, Roberts W, Szatmari P, Scherer SW (2007) Contribution of SHANK3 mutations to autism spectrum disorder. *Am J Hum Genet* 81:1289-1297.
- Morris R (1984) Developments of a water-maze procedure for studying spatial learning in the rat. *J Neurosci Methods* 11:47-60.
- Naisbitt S, Kim E, Tu JC, Xiao B, Sala C, Valtschanoff J, Weinberg RJ, Worley PF, Sheng M (1999) Shank, a novel family of postsynaptic density proteins that binds

- to the NMDA receptor/PSD-95/GKAP complex and cortactin. *Neuron* 23:569-582.
- Nemirovsky SI, Córdoba M, Zaiat JJ, Completa SP, Vega PA, González-Morón D, Medina NM, Fabbro M, Romero S, Brun B, Revale S, Ogara MF, Pecci A, Marti M, Vazquez M, Turjanski A, Kauffman MA (2015) Whole genome sequencing reveals a de novo SHANK3 mutation in familial autism spectrum disorder. *PLoS One* 10:e0116358.
- Niciu MJ, Kelmendi B, Sanacora G (2012) Overview of glutamatergic neurotransmission in the nervous system. *Pharmacol Biochem Behav* 100:656-664.
- Nickols HH, Conn PJ (2014) Development of allosteric modulators of GPCRs for treatment of CNS disorders. *Neurobiol Dis* 61:55-71.
- Okabe S (2007) Molecular anatomy of the postsynaptic density. *Mol Cell Neurosci* 34:503-518.
- Perroy J, Raynaud F, Homburger V, Rousset MC, Telley L, Bockaert J, Fagni L (2008) Direct interaction enables cross-talk between ionotropic and group I metabotropic glutamate receptors. *J Biol Chem* 283:6799-6805.
- Peters DG, Yatsenko SA, Surti U, Rajkovic A (2015) Recent advances of genomic testing in perinatal medicine. *Semin Perinatol* 39:44-54.
- Peça J, Feliciano C, Ting JT, Wang W, Wells MF, Venkatraman TN, Lascola CD, Fu Z, Feng G (2011) Shank3 mutant mice display autistic-like behaviours and striatal dysfunction. *Nature* 472:437-442.
- Phelan K, McDermid HE (2012) The 22q13.3 Deletion Syndrome (Phelan-McDermid Syndrome). *Mol Syndromol* 2:186-201.
- Phelan MC, Rogers RC, Saul RA, Stapleton GA, Sweet K, McDermid H, Shaw SR, Claytor J, Willis J, Kelly DP (2001) 22q13 deletion syndrome. *Am J Med Genet* 101:91-99.
- Pignatelli M, Piccinin S, Molinaro G, Di Menna L, Riozzi B, Cannella M, Motolese M, Vetere G, Catania MV, Battaglia G, Nicoletti F, Nisticò R, Bruno V (2014) Changes in mGlu5 receptor-dependent synaptic plasticity and coupling to homer proteins in the hippocampus of Ube3A hemizygous mice modeling angelman syndrome. *J Neurosci* 34:4558-4566.
- Pisani A, Gubellini P, Bonsi P, Conquet F, Picconi B, Centonze D, Bernardi G, Calabresi P (2001) Metabotropic glutamate receptor 5 mediates the potentiation

- of N-methyl-D-aspartate responses in medium spiny striatal neurons. *Neuroscience* 106:579-587.
- Reger DL, Foley EA, Watson RP, Pellechia PJ, Smith MD, Grandjean F, Long GJ (2009) Monofluoride bridged, binuclear metallacycles of first row transition metals supported by third generation bis(1-pyrazolyl)methane ligands: unusual magnetic properties. *Inorg Chem* 48:10658-10669.
- Ronesi JA, Collins KA, Hays SA, Tsai NP, Guo W, Birnbaum SG, Hu JH, Worley PF, Gibson JR, Huber KM (2012) Disrupted Homer scaffolds mediate abnormal mGluR5 function in a mouse model of fragile X syndrome. *Nat Neurosci* 15:431-440, S431.
- Rook JM, Noetzel MJ, Pouliot WA, Bridges TM, Vinson PN, Cho HP, Zhou Y, Gogliotti RD, Manka JT, Gregory KJ, Stauffer SR, Dudek FE, Xiang Z, Niswender CM, Daniels JS, Jones CK, Lindsley CW, Conn PJ (2013) Unique signaling profiles of positive allosteric modulators of metabotropic glutamate receptor subtype 5 determine differences in in vivo activity. *Biol Psychiatry* 73:501-509.
- Rook JM, Xiang Z, Lv X, Ghoshal A, Dickerson JW, Bridges TM, Johnson KA, Foster DJ, Gregory KJ, Vinson PN, Thompson AD, Byun N, Collier RL, Bubser M, Nedelcovych MT, Gould RW, Stauffer SR, Daniels JS, Niswender CM, Lavreysen H, Mackie C, Conde-Ceide S, Alcazar J, Bartolomé-Nebreda JM, Macdonald GJ, Talpos JC, Steckler T, Jones CK, Lindsley CW, Conn PJ (2015) Biased mGlu5-Positive Allosteric Modulators Provide In Vivo Efficacy without Potentiating mGlu5 Modulation of NMDAR Currents. *Neuron* 86:1029-1040.
- Rosenbrock H, Kramer G, Hobson S, Koros E, Grundl M, Grauert M, Reymann KG, Schröder UH (2010) Functional interaction of metabotropic glutamate receptor 5 and NMDA-receptor by a metabotropic glutamate receptor 5 positive allosteric modulator. *Eur J Pharmacol* 639:40-46.
- Sala C, Piëch V, Wilson NR, Passafaro M, Liu G, Sheng M (2001) Regulation of dendritic spine morphology and synaptic function by Shank and Homer. *Neuron* 31:115-130.
- Sala C, Vicidomini C, Bigi I, Mossa A, Verpelli C (2015) Shank synaptic scaffold proteins: keys to understanding the pathogenesis of autism and other synaptic disorders. *J Neurochem*.
- Sala M, Braida D, Lentini D, Busnelli M, Bulgheroni E, Capurro V, Finardi A, Donzelli A, Pattini L, Rubino T, Parolaro D, Nishimori K, Parenti M, Chini B (2011)

- Pharmacologic rescue of impaired cognitive flexibility, social deficits, increased aggression, and seizure susceptibility in oxytocin receptor null mice: a neurobehavioral model of autism. *Biol Psychiatry* 69:875-882.
- Sarasua SM, Boccuto L, Sharp JL, Dwivedi A, Chen CF, Rollins JD, Rogers RC, Phelan K, DuPont BR (2014) Clinical and genomic evaluation of 201 patients with Phelan-McDermid syndrome. *Hum Genet* 133:847-859.
- Schmeisser MJ, Ey E, Wegener S, Bockmann J, Stempel AV, Kuebler A, Janssen AL, Udvardi PT, Shiban E, Spilker C, Balschun D, Skryabin BV, Dieck S, Smalla KH, Montag D, Leblond CS, Faure P, Torquet N, Le Sourd AM, Toro R, Grabrucker AM, Shoichet SA, Schmitz D, Kreutz MR, Bourgeron T, Gundelfinger ED, Boeckers TM (2012) Autistic-like behaviours and hyperactivity in mice lacking ProSAP1/Shank2. *Nature* 486:256-260.
- Schmidt H, Kern W, Giese R, Hallschmid M, Enders A (2009) Intranasal insulin to improve developmental delay in children with 22q13 deletion syndrome: an exploratory clinical trial. *J Med Genet* 46:217-222.
- Schouten JP, McElgunn CJ, Waaijer R, Zwijnenburg D, Diepvens F, Pals G (2002) Relative quantification of 40 nucleic acid sequences by multiplex ligation-dependent probe amplification. *Nucleic Acids Res* 30:e57.
- Shcheglovitov A, Shcheglovitova O, Yazawa M, Portmann T, Shu R, Sebastiano V, Krawisz A, Froehlich W, Bernstein JA, Hallmayer JF, Dolmetsch RE (2013) SHANK3 and IGF1 restore synaptic deficits in neurons from 22q13 deletion syndrome patients. *Nature* 503:267-271.
- Sheng M, Hoogenraad CC (2007) The postsynaptic architecture of excitatory synapses: a more quantitative view. *Annu Rev Biochem* 76:823-847.
- Sheng M, Kim E (2000) The Shank family of scaffold proteins. *J Cell Sci* 113 ( Pt 11):1851-1856.
- Sheng M, Kim E (2011) The postsynaptic organization of synapses. *Cold Spring Harb Perspect Biol* 3.
- Soorya L, Kolevzon A, Zweifach J, Lim T, Dobry Y, Schwartz L, Frank Y, Wang AT, Cai G, Parkhomenko E, Halpern D, Grodberg D, Angarita B, Willner JP, Yang A, Canitano R, Chaplin W, Betancur C, Buxbaum JD (2013) Prospective investigation of autism and genotype-phenotype correlations in 22q13 deletion syndrome and SHANK3 deficiency. *Mol Autism* 4:18.

- Sorra KE, Harris KM (2000) Overview on the structure, composition, function, development, and plasticity of hippocampal dendritic spines. *Hippocampus* 10:501-511.
- Sykes NH, Toma C, Wilson N, Volpi EV, Sousa I, Pagnamenta AT, Tancredi R, Battaglia A, Maestrini E, Bailey AJ, Monaco AP, (IMGSAC) IMGSoAC (2009) Copy number variation and association analysis of SHANK3 as a candidate gene for autism in the IMGSAC collection. *Eur J Hum Genet* 17:1347-1353.
- Szczurowska E, Mareš P (2013) NMDA and AMPA receptors: development and status epilepticus. *Physiol Res* 62 Suppl 1:S21-38.
- Tada T, Sheng M (2006) Molecular mechanisms of dendritic spine morphogenesis. *Curr Opin Neurobiol* 16:95-101.
- Thomas NK, Wright RA, Howson PA, Kingston AE, Schoepp DD, Jane DE (2001) (S)-3,4-DCPG, a potent and selective mGlu8a receptor agonist, activates metabotropic glutamate receptors on primary afferent terminals in the neonatal rat spinal cord. *Neuropharmacology* 40:311-318.
- Tu JC, Xiao B, Naisbitt S, Yuan JP, Petralia RS, Brakeman P, Doan A, Aakalu VK, Lanahan AA, Sheng M, Worley PF (1999) Coupling of mGluR/Homer and PSD-95 complexes by the Shank family of postsynaptic density proteins. *Neuron* 23:583-592.
- Uchino S, Waga C (2013) SHANK3 as an autism spectrum disorder-associated gene. *Brain Dev* 35:106-110.
- Verpelli C, Carlessi L, Bechi G, Fusar Poli E, Orellana D, Heise C, Franceschetti S, Mantegazza R, Mantegazza M, Delia D, Sala C (2013) Comparative neuronal differentiation of self-renewing neural progenitor cell lines obtained from human induced pluripotent stem cells. *Front Cell Neurosci* 7:175.
- Verpelli C, Dvoretzkova E, Vicidomini C, Rossi F, Chiappalone M, Schoen M, Di Stefano B, Mantegazza R, Broccoli V, Böckers TM, Dityatev A, Sala C (2011) Importance of Shank3 protein in regulating metabotropic glutamate receptor 5 (mGluR5) expression and signaling at synapses. *J Biol Chem* 286:34839-34850.
- Verpelli C, Schmeisser MJ, Sala C, Boeckers TM (2012) Scaffold proteins at the postsynaptic density. *Adv Exp Med Biol* 970:29-61.
- Wang X, McCoy PA, Rodriguiz RM, Pan Y, Je HS, Roberts AC, Kim CJ, Berrios J, Colvin JS, Bousquet-Moore D, Lorenzo I, Wu G, Weinberg RJ, Ehlers MD, Philpot BD, Beaudet AL, Wetsel WC, Jiang YH (2011) Synaptic dysfunction and

- abnormal behaviors in mice lacking major isoforms of Shank3. *Hum Mol Genet* 20:3093-3108.
- Wang X, Xu Q, Bey AL, Lee Y, Jiang YH (2014) Transcriptional and functional complexity of Shank3 provides a molecular framework to understand the phenotypic heterogeneity of SHANK3 causing autism and Shank3 mutant mice. *Mol Autism* 5:30.
- Wilson HL, Wong AC, Shaw SR, Tse WY, Stapleton GA, Phelan MC, Hu S, Marshall J, McDermid HE (2003) Molecular characterisation of the 22q13 deletion syndrome supports the role of haploinsufficiency of SHANK3/PROSAP2 in the major neurological symptoms. *J Med Genet* 40:575-584.
- Won H, Lee HR, Gee HY, Mah W, Kim JI, Lee J, Ha S, Chung C, Jung ES, Cho YS, Park SG, Lee JS, Lee K, Kim D, Bae YC, Kaang BK, Lee MG, Kim E (2012) Autistic-like social behaviour in Shank2-mutant mice improved by restoring NMDA receptor function. *Nature* 486:261-265.
- Zhang H, Zhang SB, Zhang QQ, Liu M, He XY, Zou Z, Sun HJ, You ZD, Shi XY (2013) Rescue of cAMP response element-binding protein signaling reversed spatial memory retention impairments induced by subanesthetic dose of propofol. *CNS Neurosci Ther* 19:484-493.

# ***INDEX***

<b>INTRODUCTION.....</b>	<b>2</b>
<b>SYNAPSES .....</b>	<b>3</b>
<b>EXCITATORY SYNAPSES .....</b>	<b>3</b>
<b>GLUTAMATE RECEPTORS.....</b>	<b>6</b>
IONOTROPIC RECEPTORS .....	6
METABOTROPIC RECEPTORS .....	8
POSITIVE ALLOSTERIC MODULATORS (PAMs) OF mGlu5 RECEPTORS.....	11
<b>SCAFFOLD PROTEINS.....</b>	<b>12</b>
SHANKs .....	12
HOMER PROTEINS .....	15
SHANK3 ISOFORMS .....	16
<b>SHANKOPATIES.....</b>	<b>17</b>
PHELAN-MC-DERMID SYNDROME .....	18
PHELAN-MC DERMID TREATMENTS.....	20
<b>SHANK3 MOUSE MODELS .....</b>	<b>21</b>
<b>AIM OF THE STUDY .....</b>	<b>25</b>
<b>MATERIALS AND METHODS.....</b>	<b>28</b>
<b>RESULTS .....</b>	<b>39</b>
Deletion of Exon 11 of <i>SHANK3</i> gene causes ASD-like behaviors in mice.....	40
Shank3 absence alters Homer and mGlu5 synaptic localization .....	41
Shank3 absence impairs mGlu5-mediated intracellular calcium release.....	42
The effect of mGlu5 stimulation on NMDA responses in striatal medium spiny neurons is dependent on Shank3 .....	44
CDPPB is able to rescue ASD-like behaviors in <i>Shank3<math>\Delta</math>11</i> <sup>-/-</sup> mice .....	45
Shank3 absence causes alterations of Homer localization in neurons derived from patients affected by Phelan McDermid Syndrome (PMS).....	46
<b>FIGURES.....</b>	<b>48</b>
<b>DISCUSSION.....</b>	<b>62</b>
<b>REFERENCES .....</b>	<b>67</b>
<b>INDEX.....</b>	<b>79</b>